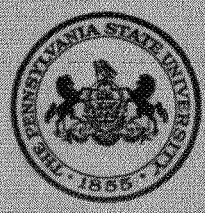


N 71 11964  
CR 111416



THE PENNSYLVANIA  
STATE UNIVERSITY

# IONOSPHERIC RESEARCH

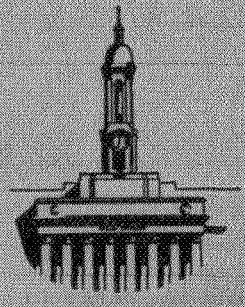
Scientific Report No. 364

Diurnal Variation of the Neutral Temperature Profile  
at Arecibo from Incoherent Scatter Measurements  
and its Relevance to the 1400 Hour Density Maximum

CASE FILE  
COPY

by  
W. E. Swartz  
October 15, 1970

IONOSPHERE RESEARCH LABORATORY



University Park, Pennsylvania    NASA Grant NGL 39-009-003



Ionospheric Research  
NASA Grant NGL 39-009-003

Scientific Report

on

Diurnal Variation of the Neutral Temperature Profile at Arecibo  
from Incoherent Scatter Measurements and its Relevance  
to the 1400 Hour Density Maximum

by


W. E. Swartz

October 15, 1970

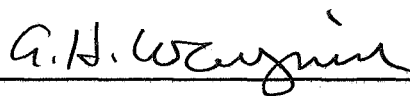
Scientific Report No. 364

Ionosphere Research Laboratory

Submitted by:

  
\_\_\_\_\_  
John S. Nisbet, Professor of Electrical Engineering  
Project Supervisor

Approved by:

  
\_\_\_\_\_  
A. H. Waynick, Director  
Ionosphere Research Laboratory

The Pennsylvania State University  
College of Engineering  
Department of Electrical Engineering

## TABLE OF CONTENTS

Abstract . . . . .	i
1. INTRODUCTION . . . . .	1
1.1 General Statement of the Problem . . . . .	
1.2 Previous Related Studies . . . . .	2
1.2.1 Satellite Orbital Decay Density Measurements . . . . .	2
1.2.2 EUV Spectrometric Density Measurements . . . . .	5
1.2.3 Mass Spectrometric Density Measurements . . . . .	8
1.2.4 Falling Sphere Density Measurements . . . . .	10
1.2.5 Theoretical Models of the Neutral Atmosphere . . . . .	11
1.2.6 Neutral Temperatures Deduced from Incoherent Scatter Observations . . . . .	17
1.3 Specific Statement of the Problem. . . . .	18
1.3.1 Temperature and Density Phase Differences . . . . .	18
1.3.2 Neutral Models Based on Incoherent Scatter Data . . . . .	18
1.3.3 Energy Transport in the Upper Atmosphere . . . . .	19
1.3.4 Error Considerations. . . . .	19
2. METHOD OF THE ANALYSIS . . . . .	20
2.1 Plasma Temperatures in the Molecular to Atomic Oxygen Ion Transition Region . . . . .	20
2.2 Formulation of the Neutral Model . . . . .	21
2.3 Neutral Heat Conduction and Thermal Column Content . . . . .	24
3. RESULTS OF THE ANALYSIS . . . . .	26
3.1 Diurnal Variation of the Exospheric Temperature and its Sensitivity on the Assumed Boundary Density . . . . .	26
3.2 Temperature Variations at the Lower Boundary . . . . .	31
3.3 Temperature Gradient Variations at the Lower Boundary and the Diurnal Density Variations . . . . .	34
3.4 Diurnal Variation of the Heat Conduction through the 120 Km Boundary, and of the Thermal Energy Column Content . . . . .	40

4.	CONCLUSIONS . . . . .	46
4.1	The Diurnal Variations of the Upper Atmosphere . . .	46
4.2	Neutral Models Consistent with Incoherent Scatter Data . . . . .	47
4.3	The Energy Budget of the Model . . . . .	47
4.4	Suggestions for Further Work . . . . .	48
	BIBLIOGRAPHY . . . . .	51

## ABSTRACT

Series of high resolution electron and ion temperature and electron density measurements at Arecibo have been used to derive profiles of the neutral temperature from 116 km to 400 km throughout the day. In this technique use was made of least square fitting to calculate a smooth temperature profile and a neutral atmospheric model. The availability of a complete profile allows calculation of the thermal energy storage and downward heat conduction throughout the day.

Two methods have been employed to calculate the density profile. The first assumes that the density at 120 km is known and solves for the diffusion equilibrium model that best fits the data. The second method requires only the assumption of the relative densities of the neutral constituents at the lower boundary but has a somewhat higher experimental variance.

It is shown that density and temperature do not in general peak at the same time as indicated by the current atmospheric models such as CIRA (1965). These models are based mainly on satellite orbital decay measurements and indicate a density maximum around 1400 hours. Neutral temperatures derived from incoherent sounding have indicated a temperature maximum near 1600 hours. It is now suggested that these two phenomena may be self consistent when the entire temperature profile affecting the neutral density is considered.

## 1. INTRODUCTION

### 1.1 General Statement of the Problem

Early solutions of the thermal continuity equation under quasi-static conditions by Harris and Priester (1962a) predicted an exospheric temperature and density maxima near 1700 hours rather than at the observed density maximum at 1400 hours. Using an additional hypothetical "second heat source" the theoretical timing of the maxima of both temperature and density were moved to 1400 hours, forcing their neutral model densities to follow those obtained from satellite orbital decay measurements. Current atmospheric models such as CIRA 1965 and the proposed "CIRA 1970" still reflect this identical phasing of the density and temperature maxima even though Nisbet (1967), Carru, Petit, Vasseur and Waldeufel (1967), and McClure (1969) have shown that the neutral temperature maximum is rather later nearer to sunset based on incoherent scatter sounding.

This difference is quite important as it has considerable bearing on the assumptions that affect calculations of atmospheric heat inputs and the effects of horizontal transport on the upper atmosphere. Later theories have attempted to reconcile the discrepancy by introducing horizontal transport. However, none to date have correctly described all of the observed phenomena.

Since the temperature and density can only be uniquely specified in a theoretical model when the distribution of energy input is known exactly, it was of interest to examine the complete measured temperature profiles and determine the implied diurnal characteristics of the temperature, density and energy storage.

## 1.2 Previous Related Studies

### 1.2.1 Satellite Orbital Decay Density Measurements

The study of the orbital decay of satellites since the launching of the first Soviet Sputnik in 1957 has provided a wealth of information about the neutral densities in the upper atmosphere. This contraction of the orbit results from a loss of total energy from the work done on the satellite by a drag force given by

$$\vec{F} = \frac{1}{2} \rho A C_D \vec{v} \vec{v}$$

where  $\rho$  is the atmospheric density.

$\vec{v}$  is the velocity of the satellite relative to the air.

$A$  is the cross sectional area of the satellite normal to  $\vec{v}$ .

$C_D$  is the drag coefficient.

For elliptic orbits the decrease in total energy results in a significant lowering of the apogee height corresponding to only a small change in perigee height. As the orbit contracts, the period decreases, while the average velocity increases until re-entry. Measurements of the period for successive passes give the rate of change of the orbital period from which the total work done by the drag force may be determined. Since the total work done on the satellite is related to the integral of the density along the entire path of the orbit rather than the density at one specific location, models of the density distribution are necessary for reducing the data. However, since the density rapidly decreases with increasing altitude, the drag force is strongest near perigee and for highly elliptic orbits produces

negligible drag for all but a small path arc of  $30^\circ$  or so about perigee (King-Hele, 1966). Detailed descriptions concerning the theory of atmospheric drag on satellites have been given by Jastrow and Pearse (1957), Sterne (1958), Krassovsky (1959), Cook et. al. (1960, 1961), King-Hele (1964, 1966), and Cook (1965, 1966).

For orbits with an eccentricity greater than 0.02, the data is usually reduced to the density at half a scale height above perigee. This minimizes the standard deviation in the errors resulting from the assumed model for which a 25% error in the scale height estimate only produces a 1% error in the density (King-Hele, 1966). Since the cross sectional area, mass and velocity of the satellite may usually be measured quite accurately, the main uncertainty in the density comes from uncertainty in the drag coefficient. Although  $C_D$  is altitude dependent, Cook (1965, 1966) has shown that use of a constant drag coefficient in the altitude range between 140 and 400 km. during low solar activity and between 140 and 600 km. during high solar activity should not introduce any appreciable errors. However, he felt that the value of  $C_D = 2.2$  usually used in drag analysis may be 10 to 15 percent too low. The paddlewheel satellite measurements of Moe (1966, 1968) also imply higher values. King-Hele (1966) has discussed the uncertainties introduced in the density estimates from orbital decay analysis and claimed that the total percentage errors in the densities can be as low as 7.6% for spherical satellites in well defined orbits. Other uncertainties in deducing boundary conditions for models based on drag measurements have been pointed out by Stein and Walker (1965).



The density distribution of the entire upper atmosphere may be obtained with the above method by using many satellites with perigees at various altitudes and geographic locations. However, the time and spacial resolution is limited by the smoothing of the density integration effect described above, and according to Moe (1970) could lead to perhaps a one hour error in the timing of the diurnal maximum. Also large transient effects can go undetected (King-Hele, 1966).

Some of the uncertainties introduced by the assumed model and by the smoothing of the density integration effect may be overcome with accelerometers mounted on the satellite (Broglio, 1967; Moe et. al., 1968; and Marcos, 1968). The major uncertainty is again the drag coefficient while calibration difficulties have posed other problems.

Another handicap of this method is that the lifetimes of satellites with perigees much less than 200 km. are very short. Only by using satellites with a very high ratio of mass to cross sectional area can the lifetimes be made long enough for useful measurements in the lower altitudes with perhaps 120 km. being the lowest possible limit (King-Hele, 1966).

A measurement technique related to orbital decay is that of the spin decay of paddlewheel satellites as described by Moe et. al. (1968) who determined variations of the density scale height over the solar cycle.

The basic diurnal behavior of the density obtained from early orbital decay measurements by Jacchia (1960), King-Hele and Walker

(1961), and by Paetzold and Zschorner (1961) with a maximum around 1400 hours and a minimum just before sunrise has remained unchanged up to the present time and shows no appreciable shift with solar activity (Jacchia, 1964).

Nicolet (1952, 1960, 1961) has shown how the vertical density distribution is related to the temperature profile and has constructed tabular models for the upper atmosphere. From such tables Jacchia (1964) was able to estimate the temperature variations using orbital decay density measurements. Refinements of such models (as will be discussed later in Section 1.2.5) have provided most of the temperatures based on orbital decay measurements. Jacchia and Slowey (1968) have warned, however, that absolute temperatures from this method are very unreliable, and their use should be restricted to only the modeling of the densities.

The correlation of density fluctuations with the solar cycle has been well established by King-Hele (1965), Jacchia (1964, 1970a, b), and by King-Hele and Quinn (1965), while Jacchia and Slowey (1964) have correlated density fluctuations with geomagnetic activity. Orbital decay analysis has revealed latitudinal and seasonal effects from the migration of diurnal bulge (Jacchia and Slowey, 1967, 1968; Newton, 1969a, b) and also a "semiannual effect" (Paetzold and Zschorner, 1961; Jacchia, 1966; and Cook, 1969).

### 1.2.2 EUW Spectrometric Density Measurements

The intensity of a given wavelength,  $\lambda$ , of solar EUV radiation at an altitude,  $Z$ , is given by

$$I(\lambda, Z) = I_0(\lambda) e^{-\sum_j \sigma_a(\lambda, j) \int n(j, Z') dS}$$

where  $I_0(\lambda)$  is the intensity of the radiation incident on the outer atmosphere.

$\sigma_a(\lambda, j)$  is the absorption cross section of the  $j^{\text{th}}$  constituent for wavelength  $\lambda$ .

$dS$  is an element of path length in the direction of the sun.

$n(j, Z)$  is the number density of the  $j^{\text{th}}$  constituent.

Rocket borne EUV spectrometers provide measurements of  $I(\lambda, Z)$  which specifies the product of the cross section and the integral of the density  $\int_Z^\infty n dS$ . If the cross section is known, differentiation of the altitude dependent measurements then provides the density profile. Reduction of the data from satellite spectrometers, however, involves a more complicated path geometry in the density integral. In this case the integral gets its main contribution in the region of closest approach to earth of the optical path.

If a measurement of  $I(\lambda, Z)$  is made for a wavelength that is selectively absorbed by only one constituent, then the number density of that particular constituent may be determined. By choosing different wavelengths which are absorbed by other constituents, densities can be obtained for even minor constituents.

Byram et. al. (1956), Hinteregger (1961), and Hall et. al. (1963, 1965) have described instruments which have been successful in making these measurements.

Rocket flights of EUV spectrometers have been described by Byram et. al. (1956), Hinteregger (1961), and Hall et. al. (1963a,



b, 1965), while Landini et. al. (1965) have described some satellite measurements.

This method has the advantage of being able to determine relative constituent compositions in addition to providing flux intensities useful in other related studies. However, the densities can be no more precise than the cross sections used to obtain them, which for active constituents may be very difficult to measure in the laboratory, and the finite spectral band pass may allow entrance of radiation with characteristics different from the main line being observed. Calibration difficulties also arise in particular with long term satellite measurements.

EUV absorption measurements leading to densities in the upper atmosphere have been made by Byram et. al. (1956), Hinteregger et. al. (1965), Landini et. al. (1965), Thomas et. al. (1965), and Hall et. al. (1967). For example, Hall et. al. (1967) chose wavelengths which were selectively absorbed by only certain constituents and were able to estimate the partial densities of the three major constituents in the altitude region from 150 to 240 km. Their results using the wavelengths 303.8, 629.7 and  $1206.5 \overset{\circ}{\text{A}}$  showed some variation in successive rocket flights; however, the atomic oxygen densities were generally greater than the corresponding CIRA (1965) model while the molecular nitrogen densities were somewhat lower.

Although the presence of a small magnetic storm or possible dependence on geographic or magnetic latitude may have influenced their conclusions, the results of Thomas et. al. (1965) indicated large day-to-day density variations in the 120-200 km. region. Such

variations have also been observed by other recent measurements (Spencer et. al. , 1966; and Pokhunkov, 1968 - see Section 1.2.3; and Champion, 1968 - see Section 1.2.4).

### 1.2.3 Mass Spectrometer Density Measurements

Mass spectrometers mounted on both rockets and satellites have provided data on atmospheric composition and temperature. Several mass spectrometers and their use in the upper atmosphere have been described by Schaefer and Nichols (1961), Spencer and Reber (1963), Spencer et. al. (1965), Hedin and Nier (1965), and Mauersberger et. al. (1968). Generally these instruments admit the neutral gas into an ionizing chamber and then separate the different constituents using carefully adjusted electric and magnetic fields. The different ions impinge upon detectors at different locations or at different times depending on their mass and the particular instrument configuration producing electric currents proportional to the density of the particular constituent. Such measurements can have a very good height resolution. It is, however, difficult to obtain absolute calibrations of the instruments especially for active constituents such as atomic oxygen.

In order to study the effects of particle collisions with the instrument walls, Hedin and Nier (1966) flew three mass spectrometers as a single unit. One spectrometer had its ionizing region exposed to the ambient atmosphere as completely as was physically possible to minimize the particle collisions with the instrument. The other two were constructed in such a way that a large number of

collisions would occur before ionization. The spectrometer with the open ion source gave  $N_2$  densities which were up to 40% lower than those measured by the two other spectrometers. Discrepancies in the measurements of atomic oxygen were also noted. The absolute number densities of O were claimed to be correct within 25 to 50%, while errors for the inactive constituent densities were somewhat lower at around 20%.

The measurements of Hedin and Nier (1966), Krankowsky et al. (1968), Kasprzak et al. (1968), Mauersberger et al. (1968a) and other results discussed by Nier (1966) and Roemer (1969) consistently have shown densities around a factor of two less than those obtained by other methods - especially those obtained from orbital decay - and thus these results have also been smaller than the values given by most neutral models (see Section 1.2.5). In contrast to the above results, Pokhunkov (1966), and Mauersberger et al. (1968b) have reported larger densities which have not shown such a large discrepancy. Mauersberger et al. (1968b) also reported density profiles which were generally very smooth except for a pronounced irregularity near 135 km. They claimed that this irregularity could not be explained by erratic behavior of their spectrometer and tentatively concluded that it was caused by an internal gravity wave. Such localized irregularities can be very important and are very hard to detect with orbital decay analysis.

Reber (1964) and Spencer et al. (1964) have used the mass spectrometer on the Explorer XVII satellite to obtain densities from



257 to 700 km. which agree with satellite drag data to within a factor of two.

In addition to calculating the temperatures from estimates of the scale heights of the density measurements, Spencer et. al. (1965) have calculated temperatures from a modulation of the density measurements which was produced by a tumbling probe.

Spencer et. al. (1966) and Pokhunkov (1968) have obtained temperatures from mass spectrometer data revealing large changes in the temperature gradients between 150 and 200 km. which were not supported by the early models of Harris and Priester (1962a, b) and Jacchia (1964). Swenson (1969) has studied the temperature profiles from similar measurements by fitting the shape parameter as defined by Jacchia and has also found marked departures from the simple dependence of this parameter on the exospheric temperature used in Jacchia's models (Jacchia, 1964, 1969). The results implied that a modification of the temperature gradients and boundary conditions at 120 km. was necessary in the models.

#### 1.2.4 Falling Sphere Density Measurements

By ejecting a sphere from a rocket in the upper atmosphere and then measuring its velocity and acceleration as it falls, the air density may be determined from the equations of motion and the drag force equation given in Section 1.2.1. Accelerometers may be mounted within the sphere to improve the measurements of the drag component of the acceleration. This method is particularly useful in the altitude range of 30 to 120 km. The sources of error in the

density measurements are listed by Horowitz (1966) as being involved with the trajectory ( $\pm 1\%$ ), vertical wind ( $\pm 5\%$ ), drag coefficient ( $\pm 2\%$ ), and the drag acceleration ( $\pm 10\%$ ).

Champion (1968) has reported on a series of falling sphere experiments which show that the 120 km. density in summer at the tropics is lower than the value given by CIRA (1965), while in winter the density is higher. Furthermore, he has shown that a nearly isopycnic level exists near 91 km. rather than at 120 km. as used in the atmospheric models prior to Jacchia (1969).

#### 1. 2. 5 Theoretical Models of the Neutral Atmosphere

Nicolet (1952) has described the general equation relating the number density, temperature and pressure of an atmosphere of a perfect gas. This equation is

$$\frac{dp}{p} = \frac{dn}{n} + \frac{dT}{T} = - \frac{dZ}{H}$$

where  $H = \frac{kT}{mg}$  is the scale height. In the upper atmosphere where the neutral constituents are diffusively separated, each constituent with its own characteristic scale height is distributed according to the equation given above. Later Nicolet (1959a, b) used theories on the photodissociation of atomic oxygen and energy fluxes in conjunction with early rocket flight data to construct some simple models of the density and temperature of the thermosphere.

After atmospheric densities became available from orbital decay analysis, Nicolet (1960) was able to show that the atmosphere was nearly isothermal above 250 km. and constructed density tables

for the isothermal region. He also explained that the variations due to solar activity and the diurnal changes were associated with the major heating mechanism of absorption of solar EUV below 200 km. The effect of horizontal conduction in controlling the properties of the upper atmosphere was also described and implied a limiting of the latitudinal and seasonal variations. By introducing vertical conduction, Nicolet showed that neutral temperature gradients in the higher altitudes must be very small. Otherwise, a larger downward heat flow would be required than could be supplied.

By assuming the diurnal bulge to be at the same latitude as the sub-solar point but lagging in longitude by some fixed amount, Jacchia (1960) derived an empirical formula describing the densities from early satellite drag data. This early model was given as a function of the 20 cm solar flux measured at the Heinrich-Hertz Institut für Schwingungsforschung in Berlin, Germany.

Since the mean molecular mass does not remain constant in the upper atmosphere (as in CIRA 1961), all the parameters describing this region could not be determined from orbital decay analysis alone. Thus Nicolet (1961) made an additional theoretical study into the physical factors relating to scale height gradients, temperature gradients, heat conduction, and diffusion leading to a revised set of neutral density and temperature models. Although Nicolet recognized the importance of atmospheric variations in the lower regions and their effect on the boundary conditions of the heterosphere, constant boundary conditions at an altitude of 120 km were used to represent average conditions which would lead to the



observed densities of about  $4 \times 10^{-12} \text{ g cm}^{-3}$  at 200 km. These boundary conditions were given as the following:

$$\begin{aligned} T_n(120) &= 325 \text{ K} \\ n(\text{N}_2, 120) &= 5.8 \times 10^{11} \text{ cm}^{-3} \\ n(\text{O}, 120) &= 7.6 \times 10^{10} \text{ cm}^{-3} \\ n(\text{O}_2, 120) &= 1.2 \times 10^{11} \text{ cm}^{-3} \end{aligned}$$

A discussion of the selection of these boundary conditions and a detailed tabulation of the resulting densities from 120 to 500 km was given by Nicolet (1962).

Using the constant boundary conditions given by Nicolet (1961), Harris and Priester (1962a, b) solved the time dependent energy balance equation given in the following form:

$$\frac{\partial}{\partial t} \left[ K(T) \frac{\partial T}{\partial Z} \right] - \rho C_p \frac{\partial T}{\partial Z} T \int_{Z_0}^Z \frac{1}{T^2} \frac{\partial T}{\partial Z} dZ' + \sum_j Q_j(Z, t) = \rho C_p \frac{\partial T}{\partial t}$$

where  $K(T)$  is the temperature dependent conductivity.

$Q_j(Z, t)$  are the altitude and time dependent energy inputs or losses.

Initial solutions yielded temperature and density maxima near sunset contrary to satellite orbital decay measurements. In order to move the maxima to 1400 Hours, Harris and Priester introduced a second heat source with a maximum around 900 hours and with an energy comparable to the EUV contribution and theorized that the second source may originate in the solar corpuscular radiation or the solar wind. This same technique was used with an adjustment of the two energy sources to fit the densities in the CIRA (1965) model to those derived from satellite drag observations.

The "static diffusion" models of Jacchia (1964) assumed an empirical temperature profile similar to that proposed by Bates (1959) of the form

$$T_n(Z) = T_n(\infty) - [T_n(\infty) - T_n(Z_0)]e^{-S(Z - Z_0)}$$

where the shape parameter  $S$  was a simple function of only  $T_n(\infty)$ . Assuming constant boundary conditions at  $Z_0 = 120$  km, tabulated densities, which fit the orbital decay data and the assumed temperature profile, were specified in terms of the exospheric temperature. Empirical formulae were then derived to relate these exospheric temperatures and their corresponding density tables to the geographic coordinates, time of day, season of the year, and to the geomagnetic and solar activities.

Stein and Walker (1965) have fitted the density data of King-Hele (1963) to the empirical formulae of Bates (1959). They found that for a given molecular density at  $Z_0$ ,  $T_n(\infty)$  became principally a function of only the atomic oxygen density at  $Z_0$  and was nearly independent of  $T_n(Z_0)$ , while  $\tau$  was mainly a function of  $T_n(Z_0)$  being nearly independent of the boundary atomic oxygen density. They further noted that the observed densities could be matched with a wide range of boundary conditions implying that satellite orbital decay data alone is not sufficient for determining the temperature and densities at the boundary altitude.

A theoretical harmonic analysis of the upper atmosphere dynamics including the non-linear terms of the hydrodynamic and thermodynamic equations was performed by Volland (1967). By

including winds in a two dimensional model, he showed that the "second heat source" postulated by Harris and Priester (1962) was not needed to obtain the 1400 hour density maximum. The wind velocities were found to be horizontal at about  $100 \text{ m s}^{-1}$  near 300 km in the morning and afternoon, while at noon and just after midnight the velocities were vertical and reached  $100 \text{ m s}^{-1}$  only in the higher altitudes.

In a later work Volland (1970) proposed that a tidal wave from the lower regions may contribute significantly to the heating in the upper atmosphere. The tidal wave implied that the boundary conditions at 120 km could not remain constant, although his model densities agreed with those of Jacchia (1964) above 300 km and with those of Marov (1965) below 250 km.

Friedman (1967) constructed a three dimensional model using solar EUV and collisional heating as the external sources of heating. In this model the location of the temperature and density maxima changed from 1600 hours in the lower altitudes to near 1400 hours for the higher altitudes. For solstice conditions the latitude of the density and temperature maxima also varied with altitude. Since the method employed a simultaneous solution of a rather coarse set of mesh points distributed over the globe, the results at first appeared somewhat questionable. However, in a later work Friedman (1970) refined the mesh and included winds and variable boundary conditions. His results indicated that maximum wind velocities of about  $100 \text{ m s}^{-1}$  occur near 140 km and that the boundary densities must increase with increasing solar activity. Winds in the higher altitudes of the model became negligible.

Stubbe (1970) has presented a simultaneous solution of the time dependent coupled equations of motion, continuity, and heat conduction for a mixture of neutral, ion and electron gases. Assuming constant boundary conditions at 120 km the predicted diurnal variation of the temperature exhibited a maximum between 1700 and 1800 hours. Neutral gas velocities were included in the solutions which gave large velocities as high as  $600 \text{ m s}^{-1}$ . Unfortunately no detailed discussion of the diurnal behavior of the neutral density was given; however, the author implies that it was similar to Harris and Priester's late hour maximum without the second heat source.

Jacchia (1970a) is the most recent formulation of an empirical model of the neutral atmosphere. For this model the isopycnic level was lowered to 90 km and allows the densities, temperatures, and temperature gradients at 120 km to vary in phase with the exospheric temperature. The assumed temperature profile starts with a constant temperature and zero gradient at  $Z_o = 90 \text{ km}$ , and while increasing with altitude passes through an inflection point at a fixed altitude,  $Z_x$ , of 125 km. Specifically the profile is given by

$$T_n(Z) = \begin{cases} T_n(Z_x) + \sum_{m=1}^4 C_n (Z - Z_x)^m, & Z_o < Z < Z_x \\ T_n(Z_x) + A \tan^{-1} \left\{ \frac{G_x}{A} (Z - Z_x) [1 + B(Z - Z_x)^n] \right\}, & Z > Z_x \end{cases}$$

where  $G_x$  is the temperature gradient at  $Z_x$  and the coefficients  $C_m$ , A, B, and n are used to obtain a fit of the related densities to the measured data.

Jacchia (1970b) has revised the numerical coefficients used in the above work with the most significant change being much larger atomic oxygen densities. As in the Jacchia (1964) model, all known dependencies of the neutral atmosphere were incorporated in the empirical functions for the exospheric temperature.

#### 1.2.6 Neutral Temperatures Deduced from Incoherent Scatter Observations

Nisbet (1967) has described a method for calculating neutral atmospheric temperatures from measurements of the electron and ion temperatures and of the electron density. Since the main energy input to the ions comes from the ambient electrons with very little contribution from high energy photoelectrons, Nisbet was able to use measured temperatures and densities of the electrons and ions to calculate the energy input to the ions. The thermal energy equation for monatomic ions for the one dimensional case was given as

$$\frac{3}{2} \left[ \frac{\partial P_i}{\partial t} + v_i \frac{\partial P_i}{\partial Z} \right] + \frac{5}{2} P_i \frac{\partial v_i}{\partial t} + \frac{\partial}{\partial Z} (\lambda_i \frac{\partial T_i}{\partial Z}) = Q_{ei} + Q_p - Q_{in}$$

where  $P_i = n_i k T_i$

$n_i$  is the ion density.

$k$  is Boltzmann's constant.

$v_i$  is the mean ion velocity in the + Z direction.

$T_i$  is the ion temperature.

$\lambda_i$  is the thermal conductivity of the ion gas.

$Q_x$  are the energy exchange rates.

In the atomic oxygen dominated region, Nisbet solved this equation for the neutral temperature which enters the equation through  $Q_{in}$ . Estimates of the importance of molecular ions and lighter ions at the extremities of the  $O^+$  region were also included.

Using incoherent scatter data from the Arecibo Observatory, Nisbet (1967) showed that the neutral temperature above 225 km reaches a maximum between 1600 and 1800 hours. Further studies by Carru et. al. (1967) at Saint-Santin, and by McClure (1969) at Jicamarca have also shown a temperature maximum near sunset.

### 1.3 Specific Statement of the Problem

#### 1.3.1 Temperature and Density Phase Differences

Can the difference in phase between the diurnal variation of the temperature as measured by incoherent scatter and the density as measured by satellite orbital decay be resolved by a consideration of the complete temperature profile?

#### 1.3.2 Neutral Models Based on Incoherent Scatter Data

Can a self consistent model of the neutral atmospheric temperatures and densities be obtained from incoherent scatter measurements alone? What differences are there between the parameters of such a model and those now current?



### 1.3.3 Energy Transport in the Upper Atmosphere

What information do the detailed temperature profiles contain about the energy transport in the upper atmosphere and, in particular, the vertical heat conduction as it affects the energy budget above 120 km?

### 1.3.4 Error Considerations

What are the absolute errors in the estimates of the temperatures and densities from incoherent scatter data and how can these be minimized?

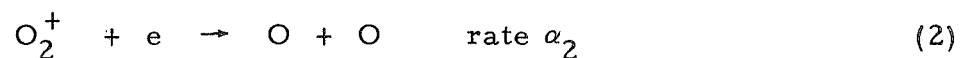
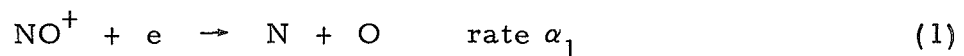
## 2. METHOD OF ANALYSIS

### 2.1 Plasma Temperatures in the Molecular to Atomic Oxygen Ion Transition Region

In the summer and winter of 1968 using an experimental technique due to Perkins and Wand, a series of high resolution measurements of backscatter autocorrelation functions was made at Arecibo. These measurements had an altitude resolution of 15 km and appeared suitable for making temperature profile measurements throughout the region from 116 km to 431 km during the day. A major difficulty with such data is that it is precisely in the region of interest that the mean ionic mass changes from that of the molecular ions  $O_2^+$  and  $NO^+$  to that of atomic oxygen.

Since the estimates of the ion and electron temperatures from the backscatter autocorrelation functions depends critically on the relative ionic densities, it was considered important to make these estimates as accurate as possible. The method employed a program due to Nisbet (1969) in which photoequilibrium theoretical models for the F1 region were calculated using estimates of the solar fluxes by Hinteregger (1967), as modified in accordance with observed changes over the solar cycle and the more recent measurements reported by Hall, Higgins, Chagnon, and Hinteregger (1969).

Reaction rates for the reactions of importance in the F-region were chosen to be

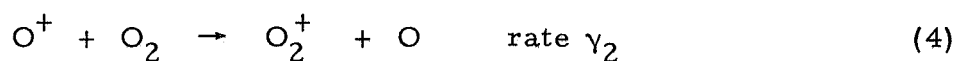
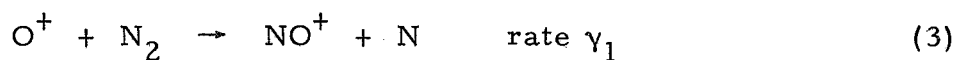


where

$$\alpha_1 = \frac{1.44 \times 10^{-4}}{T(z)} \quad \text{Weller and Biondi (1968)}$$

$$\alpha_2 = \frac{6.6 \times 10^{-5}}{T(z)} \quad \text{Kasner and Biondi (1967)}$$

and



where  $\gamma_2 = 10\gamma_1$  and  $\gamma_1$  was chosen to provide a fit with the theoretical models of the F2 region in the vicinity of the peak.

Neutral atmospheric models and in particular  $\text{N}_2$  and  $\text{O}_2$  densities were of importance to the estimates of reactions 3 and 4; however, the way in which the reaction rates  $\gamma_1$  and  $\gamma_2$  were determined was intended to minimize this effect. Neutral densities were determined using analytical fits to the CIRA 1965 models, although as will be described later, models based on observed temperature profiles were used for checking purposes later in the work. The final atomic oxygen ion percentage compositions were adjusted for differences between the theoretical and measured electron densities.

## 2.2 Formulation of the Neutral Model

Incoherent scatter measurements provide only ion and electron temperatures. Thus the methods of Nisbet (1967) were employed to calculate the neutral temperature. As shown by Nisbet the

differences between the ion and neutral temperatures are small below 225 km in the region where the molecular ions become of importance. It was therefore found convenient to estimate the differences between the ion and neutral temperatures at all heights based on the ion  $O^+$  and to merely check that the corrections were indeed negligible at lower altitudes. Setting the energy input to the ions equal to their loss and using the energy transfer rates of Banks (1966a, b) the neutral temperature may be estimated using equation (1).

$$T_n = T_i - \frac{4.8 \times 10^7 n_e (T_e - T_i)}{T_e^{3/2} \{6.6n(N_2) + 0.21(T_i + T_n)^{1/2} n(O) + 5.8n(O_2)\}} \quad (1)$$

Using the above methods, a series of neutral temperatures was obtained at the altitudes corresponding to the altitudes of the  $T_e$  and  $T_i$  measurements. To develop neutral models based on these measurements it was decided to fit the empirical formula of Bates (1959) to the observations. This formula is given by

$$T_n(Z) = T_n(\infty) - \{T_n(\infty) - T_n(Z_0)\} e^{-\tau\phi} \quad (2)$$

where  $\phi$  is the geopotential altitude given by

$$\phi = \frac{(Z - Z_0)(R + Z_0)}{R + Z}$$

in which  $R$  is the radius of the earth and  $Z_0$  the reference altitude (taken here as 120 km). With the assumption of diffusive equilibrium above  $Z_0$  this form for the temperature distribution is useful in that it leads to a convenient formula for the neutral densities:

$$n(j, Z) = n(j, Z_0) e^{\tau\phi} \left\{ \frac{T_n(Z_0)}{T_n(\infty) [e^{\tau\phi} - 1] + T_n(Z_0)} \right\}^{1 + \gamma_j} \quad (3)$$

where

$$\gamma_j = \frac{m_j g(Z_0)}{\tau k T_n(\infty)}$$

$g(Z_0)$  is the acceleration of gravity at  $Z_0$ .

$m_j$  is the  $j^{\text{th}}$  species mass.

$k$  is Boltzman's constant.

This formulation of a neutral model has been discussed by Stein and Walker (1965) who fitted equation (3) to the density data of King-Hele (1963). For satellite orbital decay data they found that for a given molecular density at  $Z_0$ ,  $T_n(\infty)$  became principally a function of only the atomic oxygen density at  $Z_0$  and was nearly independent of  $T_n(Z_0)$ , while  $\tau$  was mainly a function of  $T_n(Z_0)$  being nearly independent of the boundary atomic oxygen density. They further noted that the observed densities could be matched with a wide range of boundary conditions implying that satellite orbital decay data alone is not sufficient for determining the temperature and densities at the boundary altitude.

The use of this model is very different for incoherent scatter sounding measurements. What is available are the electron densities and electron and ion temperatures at a large number of altitudes. At the lower altitudes the ion and neutral temperatures are close to one another so that the neutral temperatures are well defined. At altitudes in excess of about 200 km the ion temperature during the day

is above the neutral temperature by an amount dependent upon the neutral density, and this may be used to make estimates of the major neutral species, atomic oxygen, independent of assumptions about the boundary conditions. For the fitting process values for the densities of atomic oxygen, molecular nitrogen and molecular oxygen at 120 km were assumed. Values of  $\tau$ ,  $T_n(Z_0)$  and  $T_n(\infty)$  were then adjusted to provide a fit to equation (1) for the neutral temperature using a least squares iteration procedure. This procedure was then repeated for varying boundary densities to minimize the squared error with respect to the atomic oxygen density at 120 km.

### 2.3 Neutral Heat Conduction and Thermal Energy Column Content

Once the neutral temperature and density profiles are specified, the neutral gas heat conduction fluxes are also specified.

Specifically the heat conduction is given by

$$F(Z) = - \bar{\lambda}_c \frac{dT_n}{dZ} \quad (5)$$

where  $\bar{\lambda}_c$  is taken to be the average of the individual conduction coefficients weighted to the relative constituent densities or

$$\bar{\lambda}_c \approx \frac{\sum_j n(j, z) \lambda(j)}{\sum_j n(j, z)}$$

Nicolet (1960) gave these coefficients as

$$\lambda(O_2) = \lambda(N_2) = 1.8 \times 10^2 T_n^{1/2} \text{ erg cm}^{-1} \text{ sec}^{-1} \text{ K}^{-1}$$

$$\lambda(O) = 3.6 \times 10^2 T_n^{1/2} \text{ erg cm}^{-1} \text{ sec}^{-1} \text{ K}^{-1}$$



The necessary derivative may be simply expressed as

$$\frac{dT_n(z)}{dz} = [T_n(\infty) - T_n(Z_0)] \tau e^{-\tau\phi} \frac{d\phi}{dz}$$

The heat flux conducted down through the reference altitude of 120 km is given by

$$F(Z_0) = -\bar{\lambda}_c \tau [T_n(\infty) - T_n(Z_0)] \quad (6)$$

Diurnal variations of the thermal energy in a vertical column above  $Z_0$  are also of interest. In general the column energy content is approximated by integrating  $c_p n k T$  upwards from  $Z_0$  for all species present. For the assumed model the energy associated with large scale mass motion was neglected and the following was used:

$$u \approx k T_n(Z_0) \sum_j \left\{ n(j, Z_0) C_p(j) \int_{Z_0}^{\infty} \left[ \frac{T_n(Z_0)}{T_n(\infty)[e^{\tau\phi} - 1] + T_n(Z_0)} \right]^{Y_j} dz \right\}$$

where  $C_p(j)$  is the specific heat at constant pressure for the  $j^{\text{th}}$  species

$k$  is Boltzmann's constant.

The integration was performed using a Gaussian numerical integration procedure.

### 3. RESULTS OF THE ANALYSIS

#### 3.1 Diurnal Variation of the Exospheric Temperature and its Sensitivity on the Assumed Boundary Density

Figure 1 shows the behavior of  $T_n(\omega)$  for two winter days and one summer day. These were calculated using the assumption that the neutral boundary densities were as given in CIRA (1965). The error bars shown are the one standard deviation limits for the mean squared error. It is apparent that in the period between 1400 and 1800 hours the calculated value of  $T_n(\omega)$  increases by roughly 20K per hour. This is in agreement with previous measurements by Nisbet (1967) at Arecibo and is opposed to the decrease in temperature of about 40K per hour given in the CIRA 1965 model. A second difference lies in the lower value of  $T_n(\omega)$  measured than would be calculated by the CIRA formula:

$$T_{14}(\omega) = 5.1\bar{F} + 690 + \left\{ \left[ 0.39 + 0.15 \sin\left(2\pi \frac{d-172}{365}\right) \right] \sin\left(4\pi \frac{d-80}{365}\right) - 0.30 \right\} \bar{F} \quad (4)$$

where  $d$  is the day number,  $\bar{F}$  the 2800 MHz flux in units of  $10^{-22} \omega/m^2$  c/s. For the days in question the relevant parameters are:

Date	$\bar{F}$		1400 hours Calculated $T(\omega)$	solar time Measured $T(\omega)$	Diff. %
	Previous Day	Given Day			
6/26/68	149.1	141.4	1406	1100	28
12/13/68	143.4	135.7	1390	1070	29
12/14/68	135.7	138.6	1351	1030	31

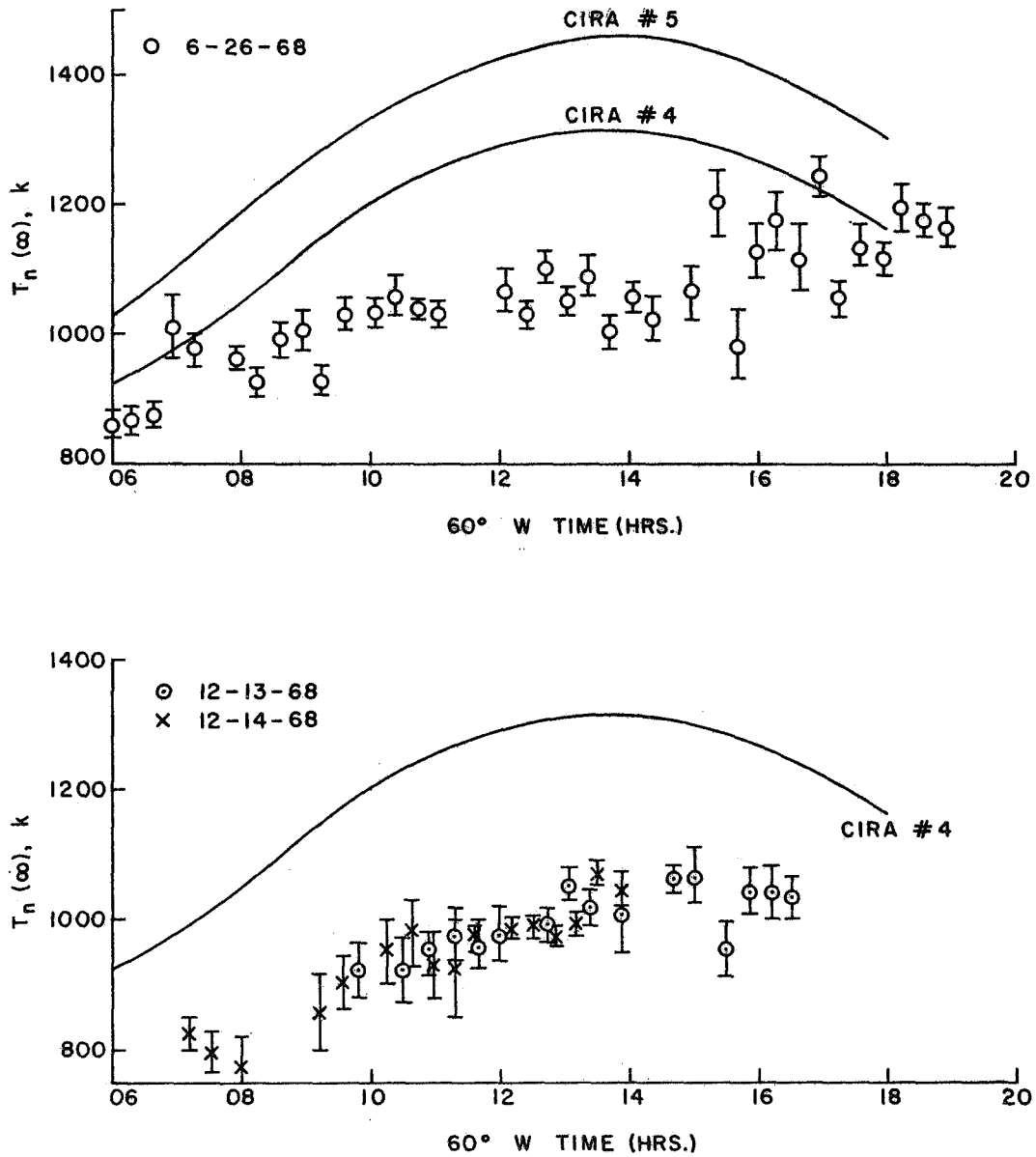


Figure 1

$T_n(\infty)$  observed at Arecibo and as predicted by the CIRA 1965 model

The above temperatures are related to the assumptions about the lower boundary conditions. The choice of the lower boundary density is not arbitrary, however, for the assumption affects the accuracy with which the temperature profile can be fitted. Figure 2A shows an example of a typical fit to the neutral temperatures as a function of altitude with the CIRA (1965) boundary densities. For figure 2B densities 50% of the CIRA (1965) values were assumed. In this case the differences between the ion and neutral temperatures become large for the higher altitudes, and negative temperature gradients result. Such negative gradients imply an upward heat conduction which would be difficult to justify theoretically and do not fit the assumed model given in equation 2. This allows a lower bound to be placed on the atomic oxygen boundary density and hence the value of  $T_n(\infty)$ .

The effect is well illustrated when the mean squared error is plotted as a function of  $n(O)_{120}$ . Figure 3 shows several examples of the way this parameter behaves. This lower bound varies with the individual measurement but for most of the profiles studied to date values of  $n(O)_{120}$  below about  $5 \times 10^{10} \text{ cm}^{-3}$  provide a poor fit to the data. It would thus seem that measurements reported by Kranowsky et. al. (1968) would be too low to be reconciled with these data unless geographical differences or perhaps departures from diffusion equilibrium in the region of 120 km are more important than are now believed. The estimates of the atomic oxygen density in the present work are based on departures of the ion temperature from the neutral temperature in the region of 300 to 400 km and hence are applicable

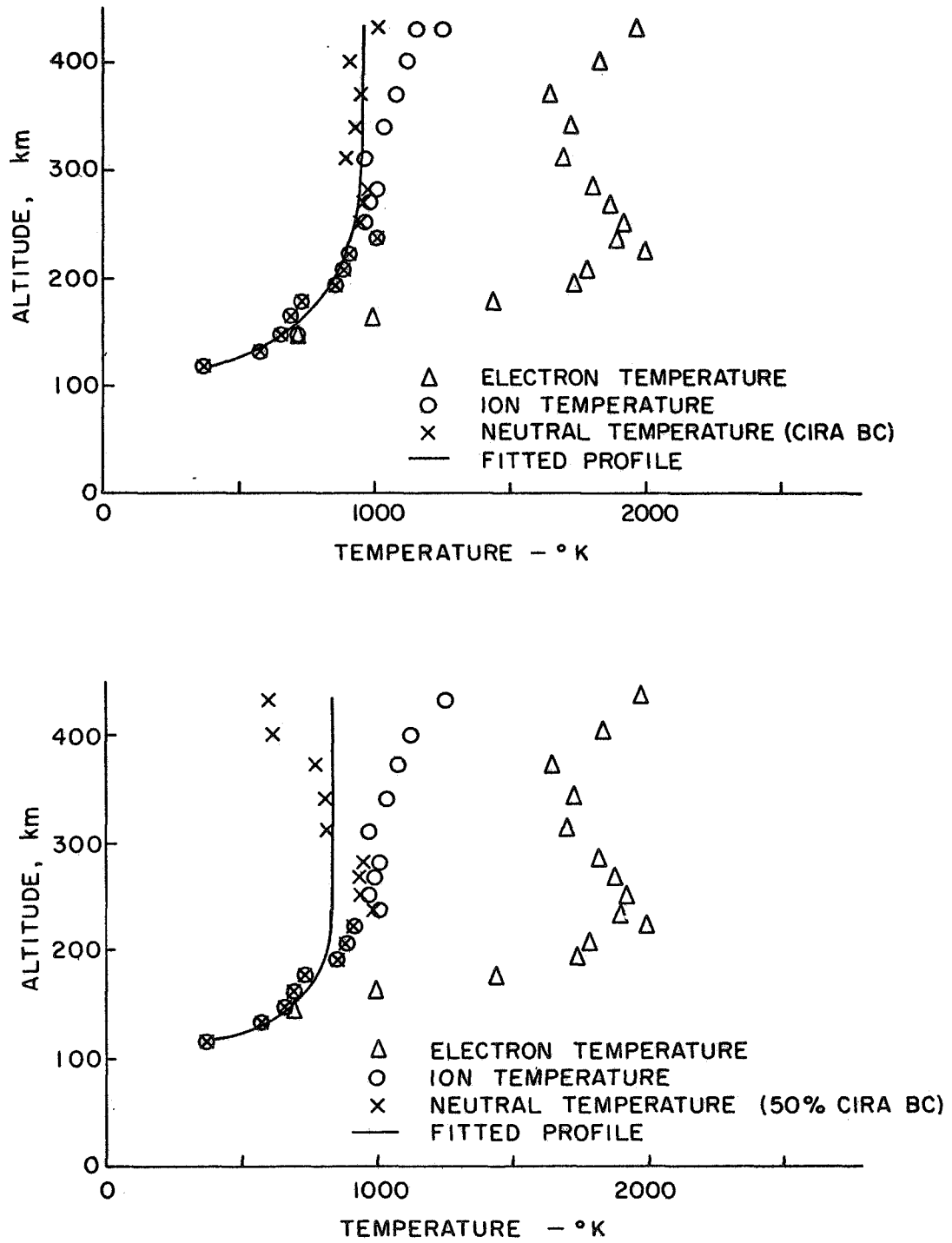


Figure 2

Typical fitted profiles: (a) using CIRA 1965 boundary densities  
(b) using 50% of the CIRA 1965 boundary densities

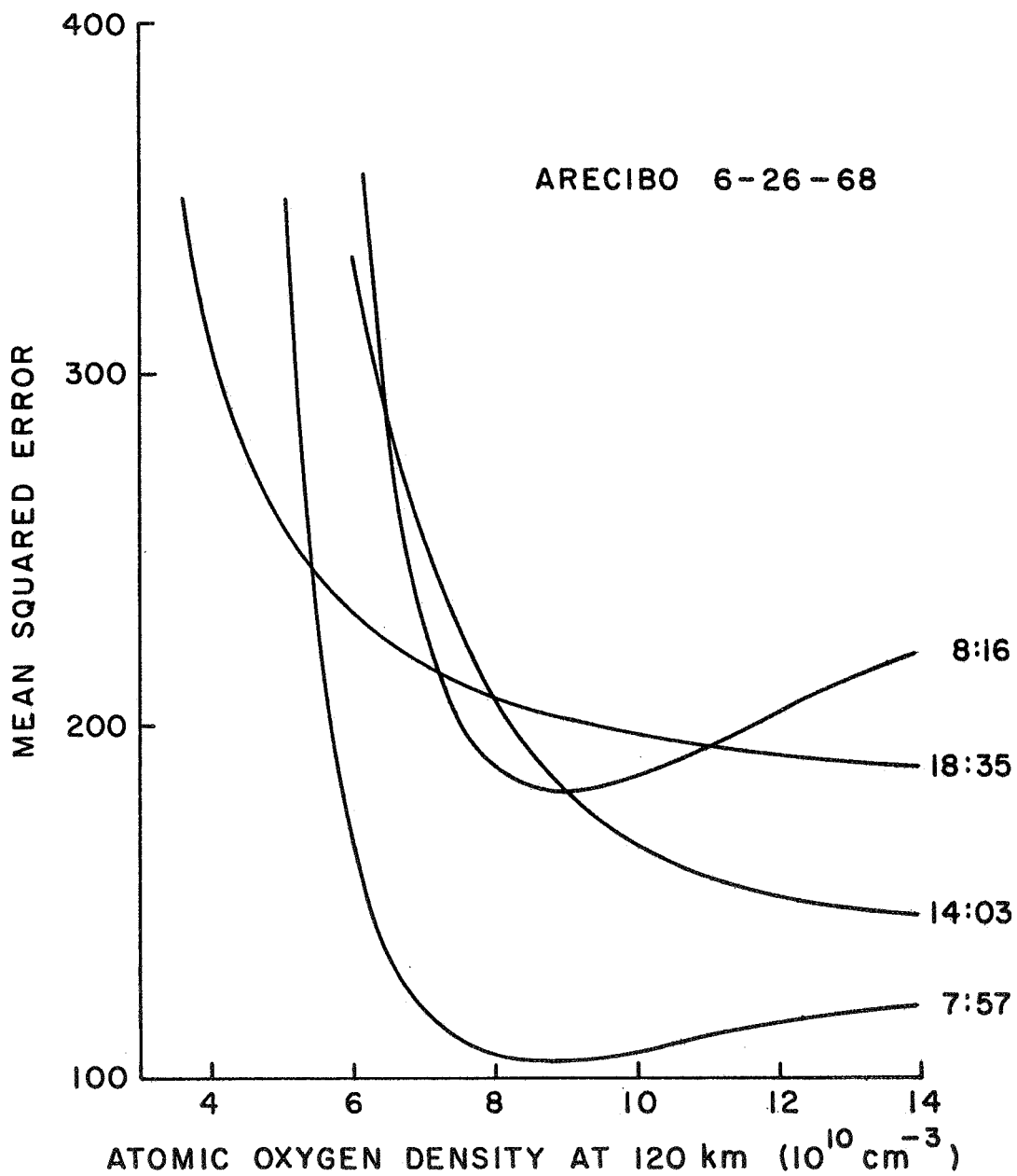


Figure 3

Effect of the boundary density on the mean squared error of the fitted profiles



to this altitude region. Estimates of the boundary densities are made by the use of the diffusion equation with the best fit neutral temperature profile.

Figure 4 shows calculated values of  $T_n(\infty)$  as a function of the boundary atomic oxygen density for three times during the day of June 26, 1968. For the calculations upon which this figure was based, the ratio of the three major constituents at 120 km were kept constant at the CIRA (1965) values. Due to the effect illustrated in Figure 2B, the fit rapidly deteriorates for the smaller assumed values of  $n(O)_{120}$ , and the points corresponding to the sum of the squared errors twice the minimum are shown with an asterisk (\*).

It is apparent that if it is accepted that the atomic oxygen density at 18:35 h was not lower than  $3.7 \times 10^{10}$  at which value the mean squared error was twice the smallest error then no matter how high the boundary density was at 14:03 hrs. the temperature must have been lower at around 14 hours than at around sunset.

### 3.2 Temperature Variations at the Lower Boundary

Figure 5 shows values of the temperature at 120 km,  $T_n(Z_o)$ , calculated from the least squares fitting program described earlier. The error bars represent the combined effect of the one standard deviation fitting error and the perturbation of the lower boundary densities by a factor of two in either direction from the CIRA (1965) values. The average value of the temperature appears to be significantly greater than the CIRA (1965) values on all three days. There does appear to be a cyclic variation in the boundary temperature with

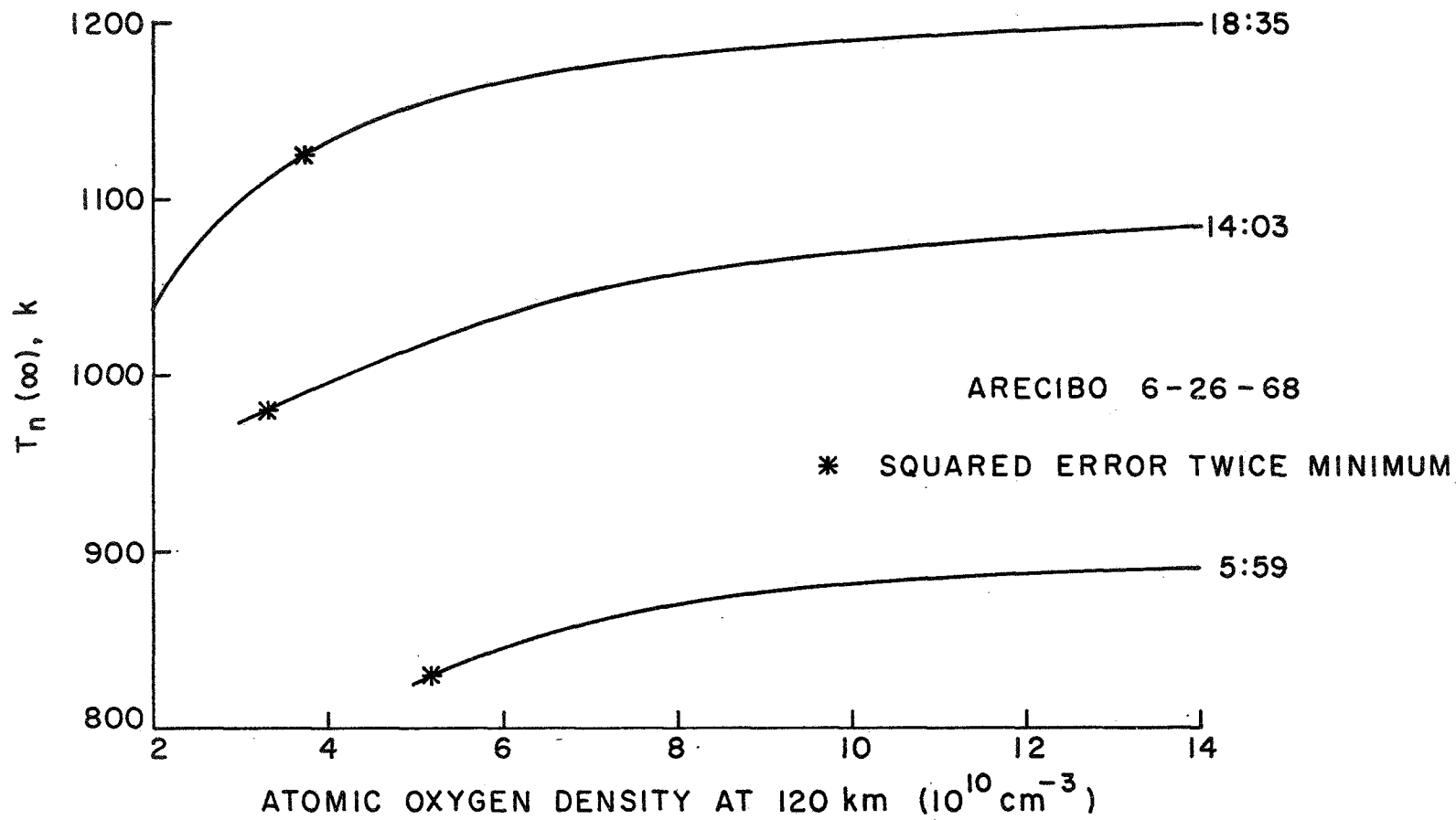


Figure 4

Effect of the boundary density on the parameter  $T_n(\infty)$  obtained from the fitting technique

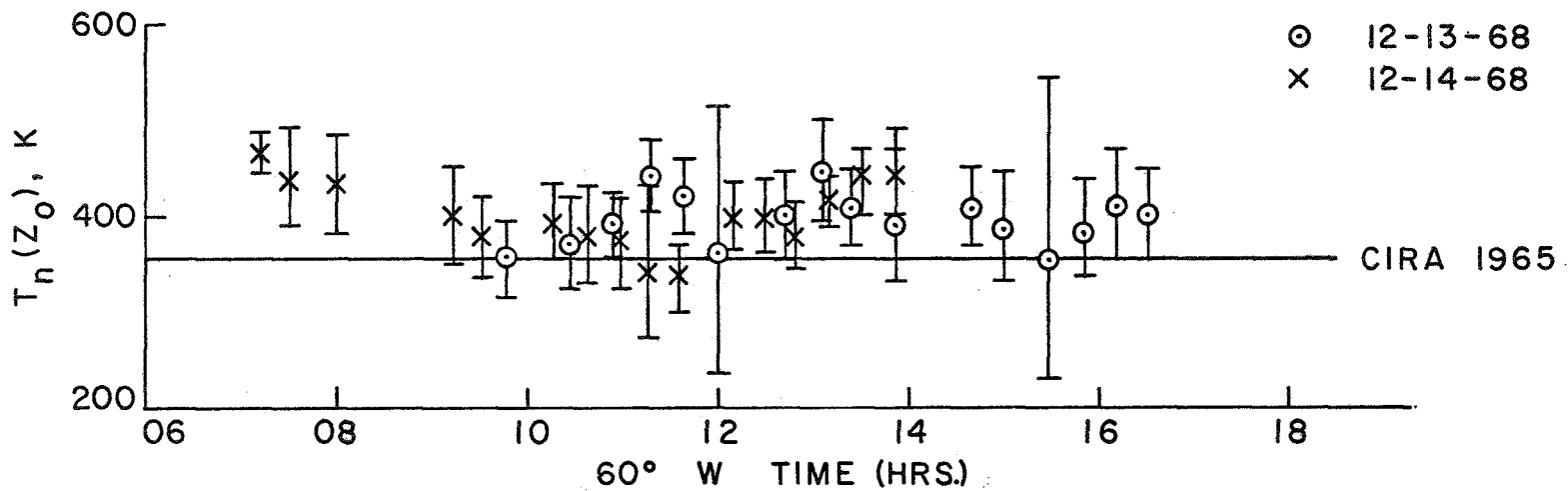
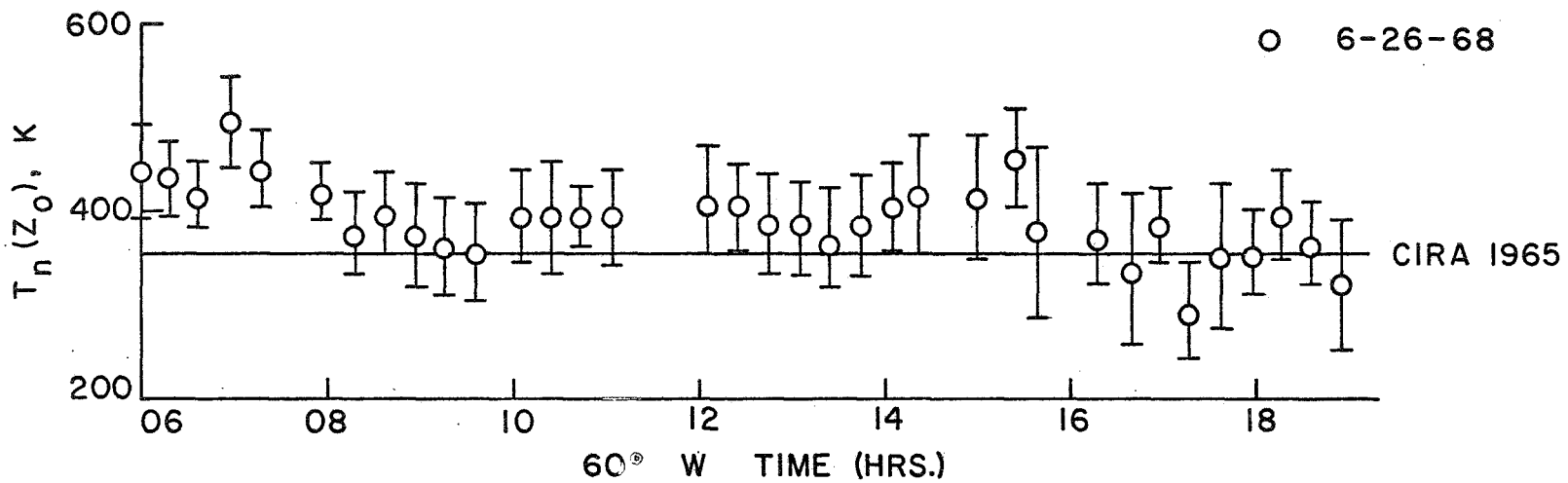


Figure 5

$T_n(Z_0)$  observed at Arecibo

a period of about four hours, but more data would be required before it could be considered to be significant. It has recently been postulated by Chandra and Stubbe (1970) that the phase difference between the density and temperature at 300 km might be explained by a modulation of the lower boundary conditions. They considered an example in which the boundary temperature at 120 km was modified by a cosine function having an amplitude of 50 K with a maximum at noon. This does not appear to be consistent with the present temperature measurements.

### 3.3 Temperature Gradient Variations at the Lower Boundary and the Implied Diurnal Density Variations

Figure 6 shows the values for the temperature gradients at 120 km,  $\frac{\partial T}{\partial Z}(Z_0)$ . The error bars again represent the combined effect of a one standard deviation fitting error and the perturbation of the lower boundary densities by a factor of two from the CIRA (1965) values. For the data of June 26, 1968 it is apparent that there is a major departure from the CIRA (1965) variation in the boundary temperature gradient from 9 to 14 hours. The variations for the December data were similar but of smaller amplitude. Since this term controls the rate of change of the scale height with increasing altitude, the gradient affects the number of scale heights between any two altitudes through the integral

$$\frac{mg}{k} \int_{z_0}^z \frac{dz}{T_n}$$

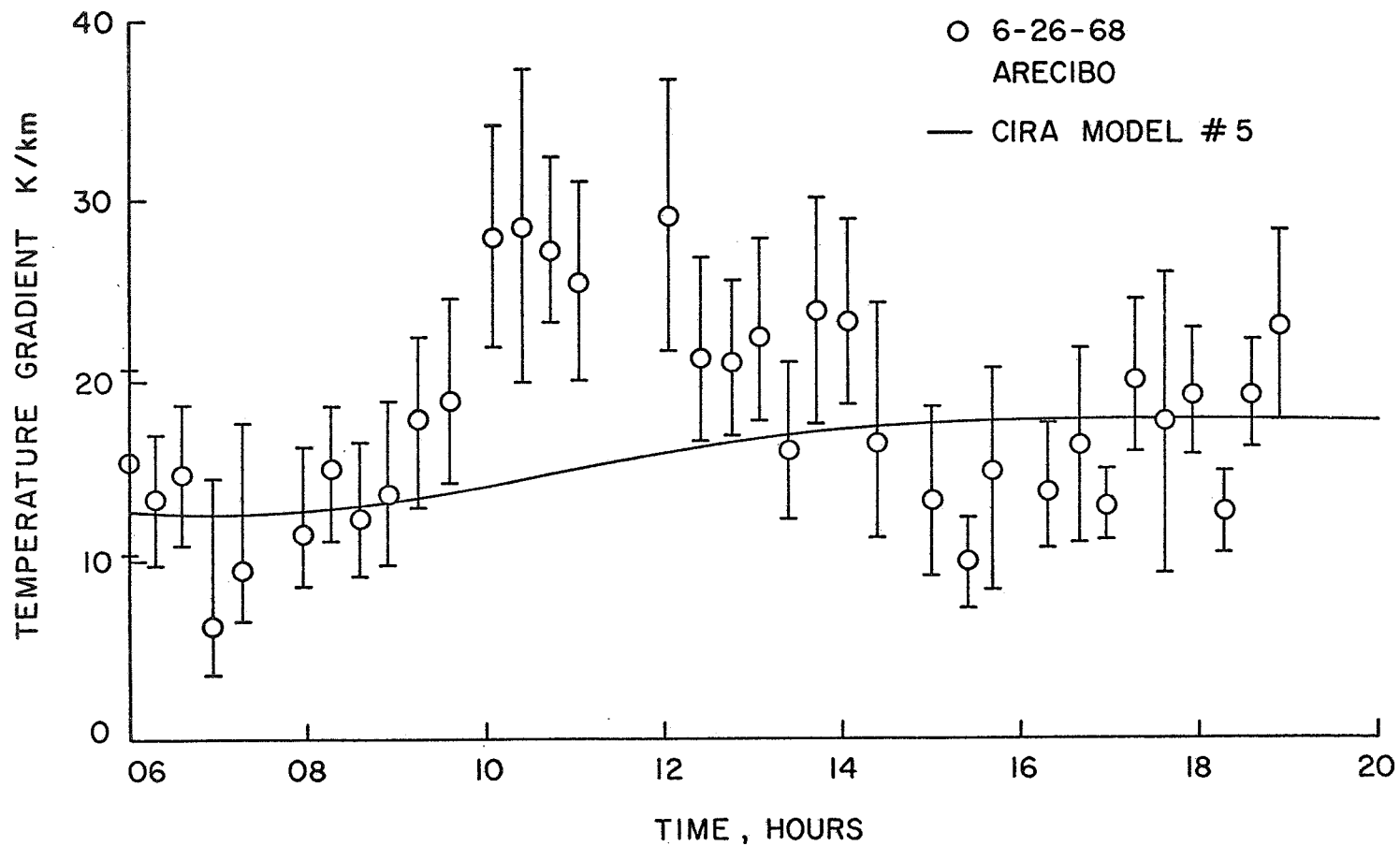


Figure 6

Diurnal variation of the temperature gradient at 120 km for June 26, 1968 at Arecibo for three different assumed boundary densities

and thus effects the ratio of the neutral densities at 300 km and at  $z_0$  in a diffusion equilibrium atmosphere.

Figures 7 and 8 show the neutral density at 300 km for June 26, 1968 and December 13-14, 1968. For these measurements the CIRA (1965) boundary densities were assumed. Error bars correspond to the one standard deviation errors in the least squares fitting procedure. It is apparent that the density maximum does not coincide with that of the temperature but occurs four to six hours earlier. It is thus apparent that the time difference between the density maximum as observed by satellite measurements and the temperature maximum as observed by incoherent scatter sounding can be explained without assuming a variable boundary density at 120 km. Furthermore, boundary densities close to CIRA (1965) values provide good agreement for the calculated and observed densities at 300 km in spite of the differences between the CIRA (1965) values of  $T(\infty)$  and those observed in this series of measurements. These differences between the observations and the CIRA (1965) model are adequately explained by differences in the temperature gradient close to 120 km.

Figure 9 shows the effect of perturbing the boundary density above and below the CIRA (1965) value. Error bars reflect the one standard deviation fitting error as associated with each profile for a given assumed boundary density. The larger boundary density gives 300 km densities far in excess of those listed in CIRA (1965) while those for the smaller boundary density are generally smaller than the CIRA (1965) values except for early morning. The relative diurnal



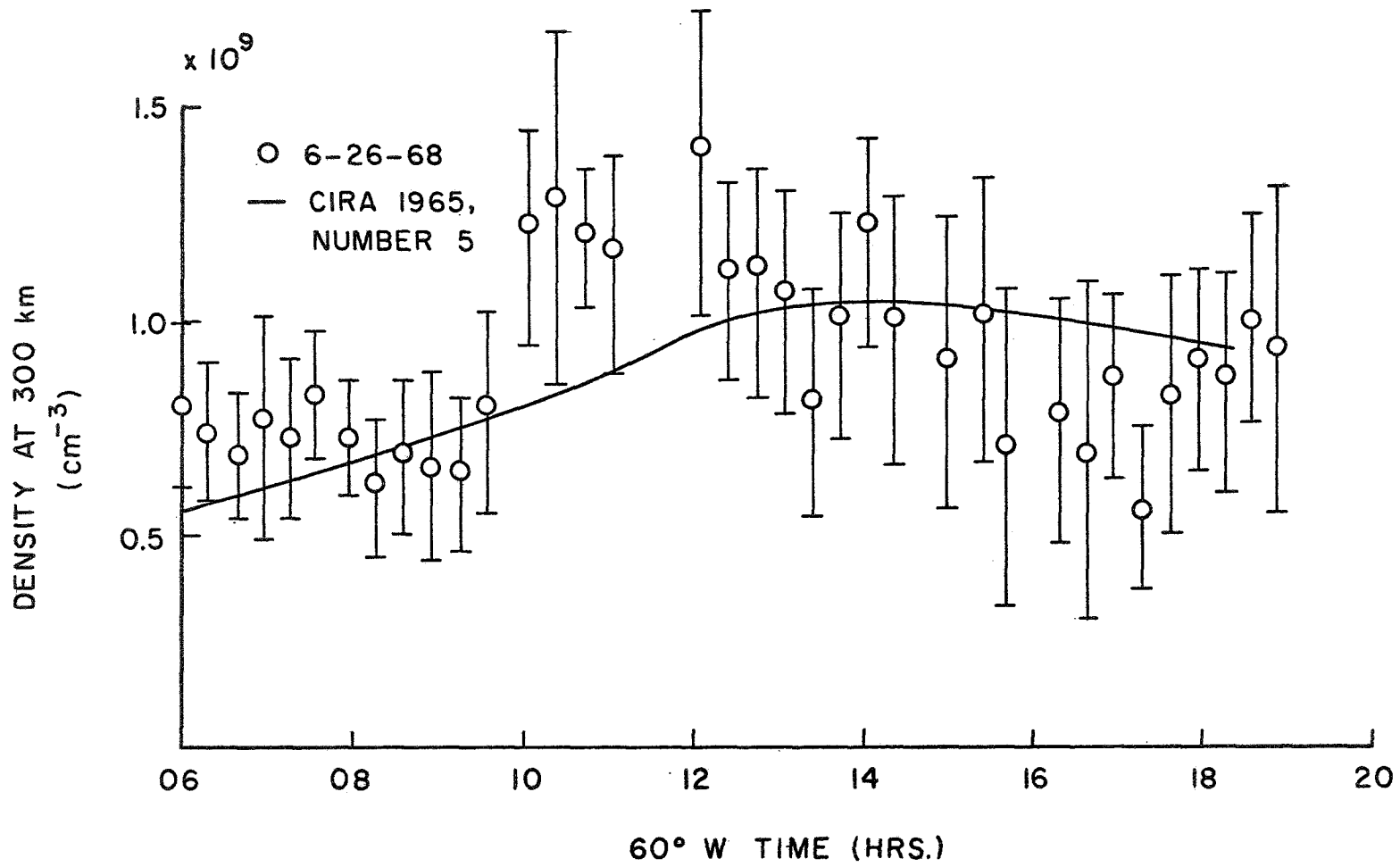


Figure 7

The diurnal variation of the 300 km density at Arecibo  
on June 26, 1968

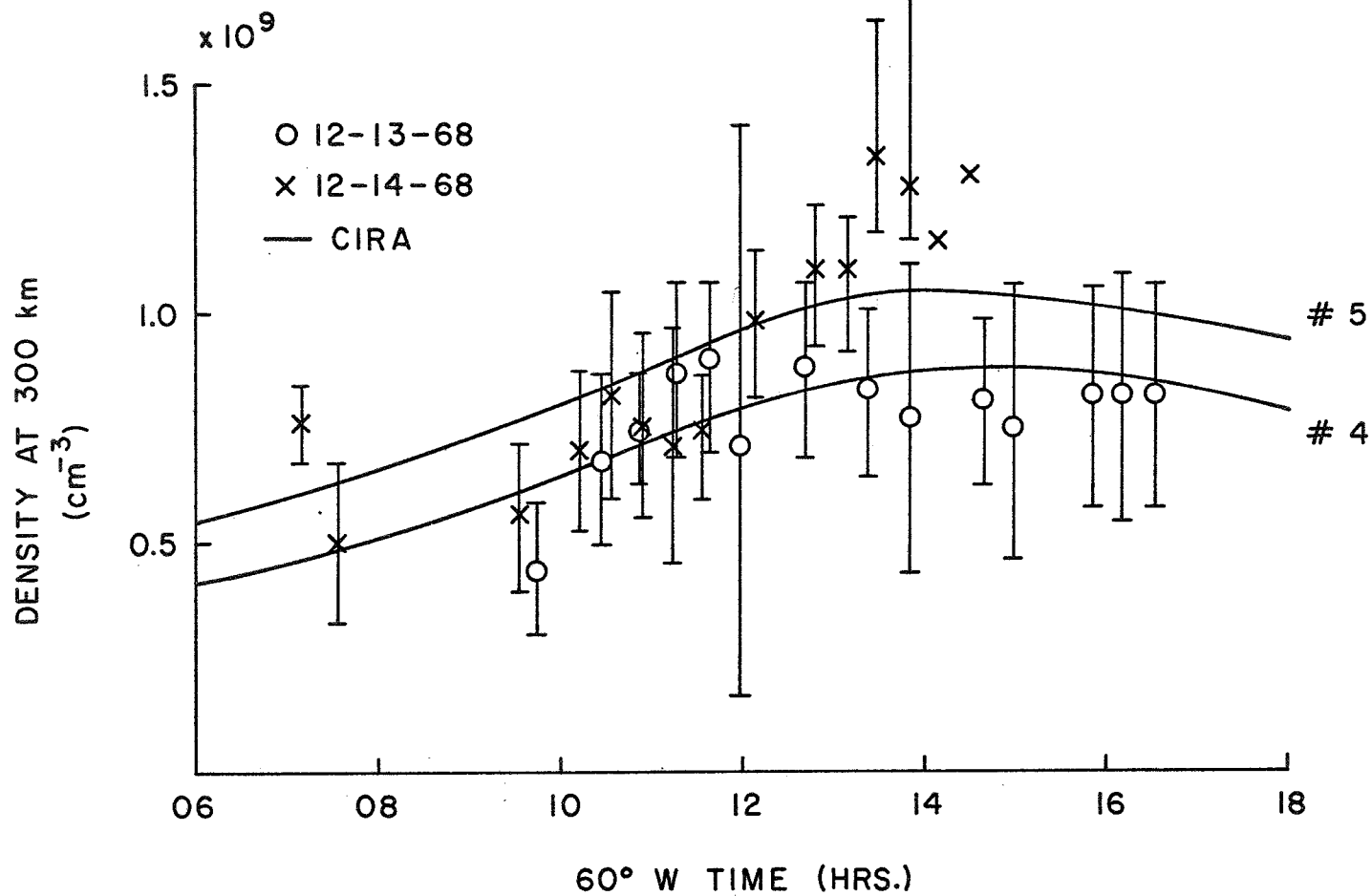


Figure 8  
 The diurnal variation of the 300 km density at Arecibo  
 on December 13 and 14, 1968

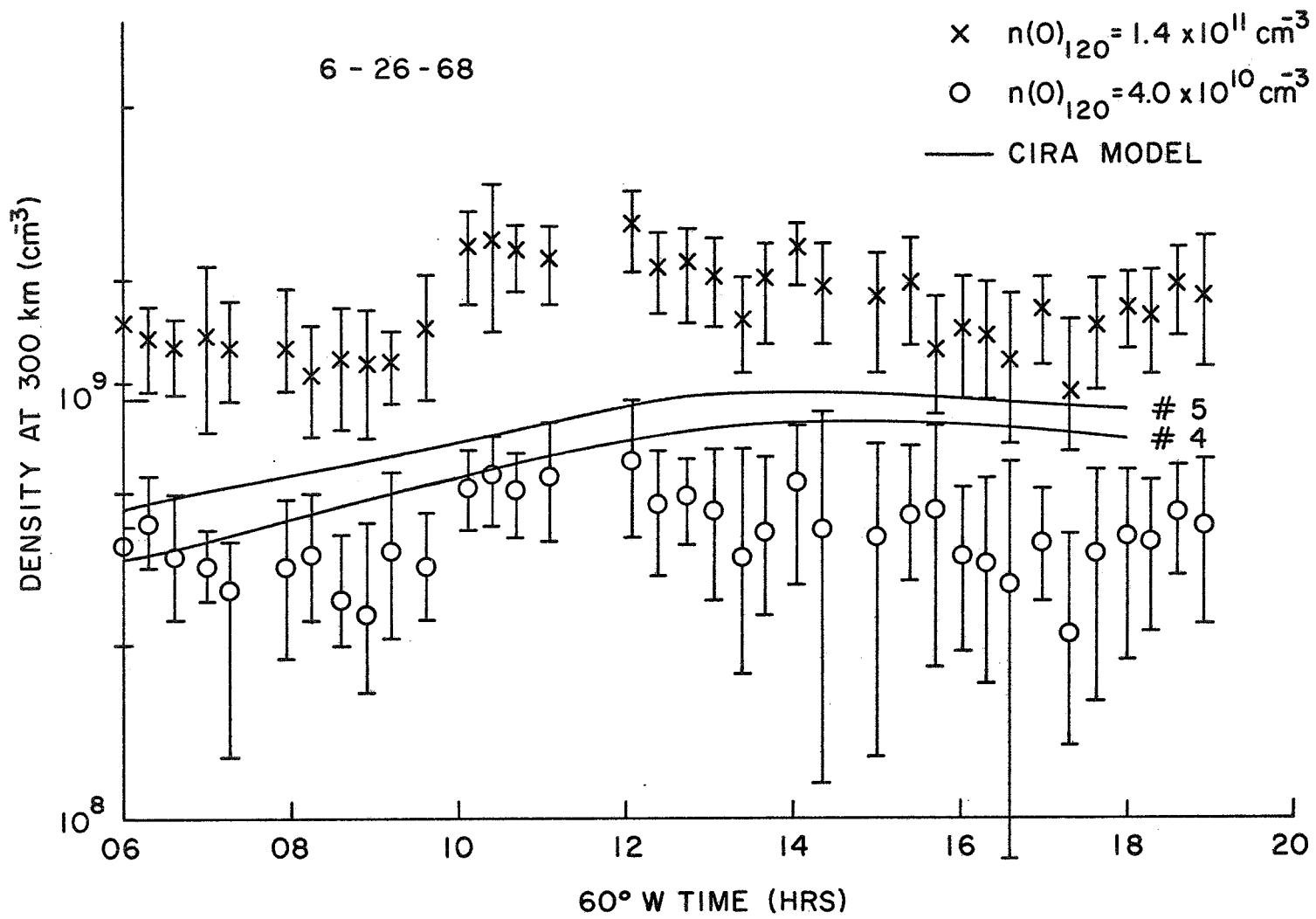


Figure 9

Effect of the boundary density on the 300 km density for June 26, 1968

variations of the 300 km densities with a maximum near mid-day are quite similar for the three different boundary densities. These curves allow the effect of a perturbation in the lower boundary densities to be estimated. If, for example, it is assumed that the density function is well known from satellite orbital decay studies then the required boundary condition at 120 km to reconcile the diffusion equilibrium assumption and the observed profile cannot depart very far from the CIRA (1965) values.

#### 3.4 Diurnal Variation of the Heat Conduction through the 120 Km Boundary and of the Thermal Energy Column Content

Figures 10 and 11 show the variation of the heat conduction for the three days data being considered here. The summer data shows an increase of more than a factor of two from 900 hours to 1200 hours, followed by a sharp decrease in the afternoon. The winter days show a similar morning increase with a more moderate afternoon decline. This may be compared with the markedly different heat conduction predicted by the CIRA model which shows a gradual increase in the conduction throughout the day to a maximum near 1800 hours.

Another quantity of interest is the heat content in a vertical column above the reference altitude. Figures 12 and 13 show the daytime changes in this term for the three days at Arecibo and compares them to the heat content predictions of the CIRA models. Again a striking difference in the general shape of the observed variations and the model may be noted.

If the conduction were to remain nearly constant throughout the night at about  $0.8 \text{ ergs per cm}^2 \text{ per sec}$ , then in the absence of a

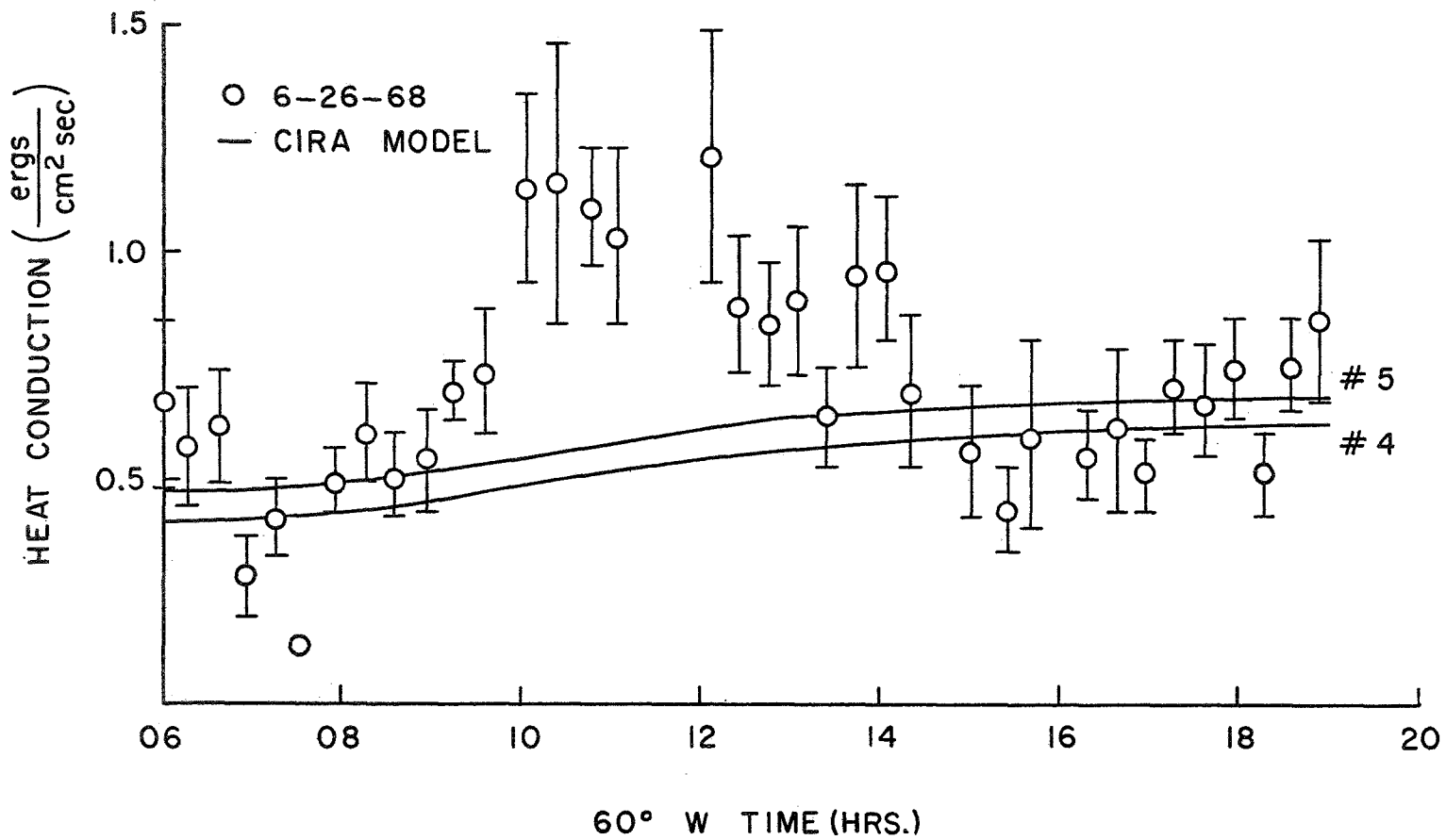


Figure 10

The heat conduction through the 120 km boundary  
for June 26, 1968 at Arcibo

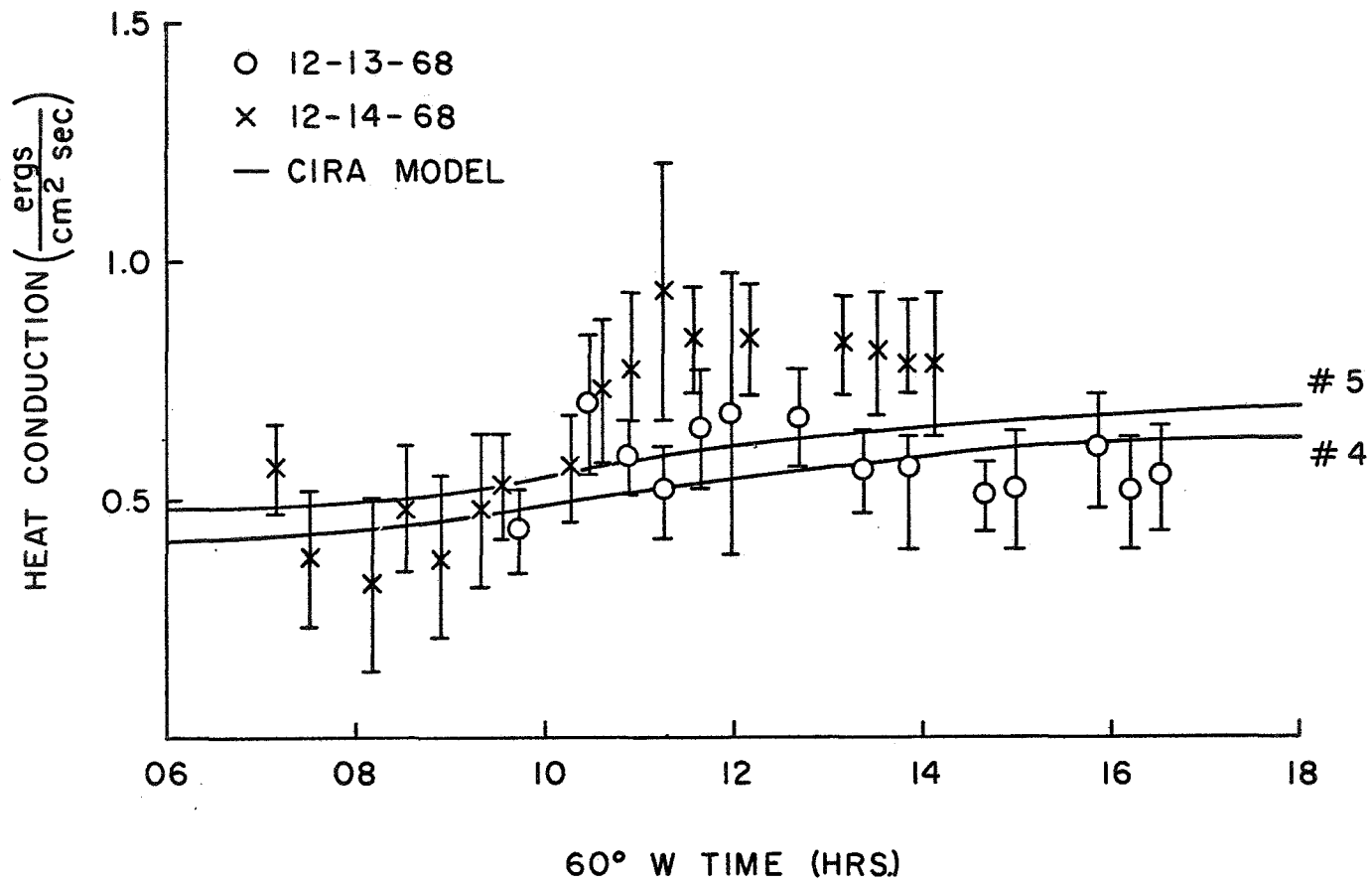


Figure 11

The heat conduction through the 120 km boundary for December 13 and 14, 1968 at Arecibo

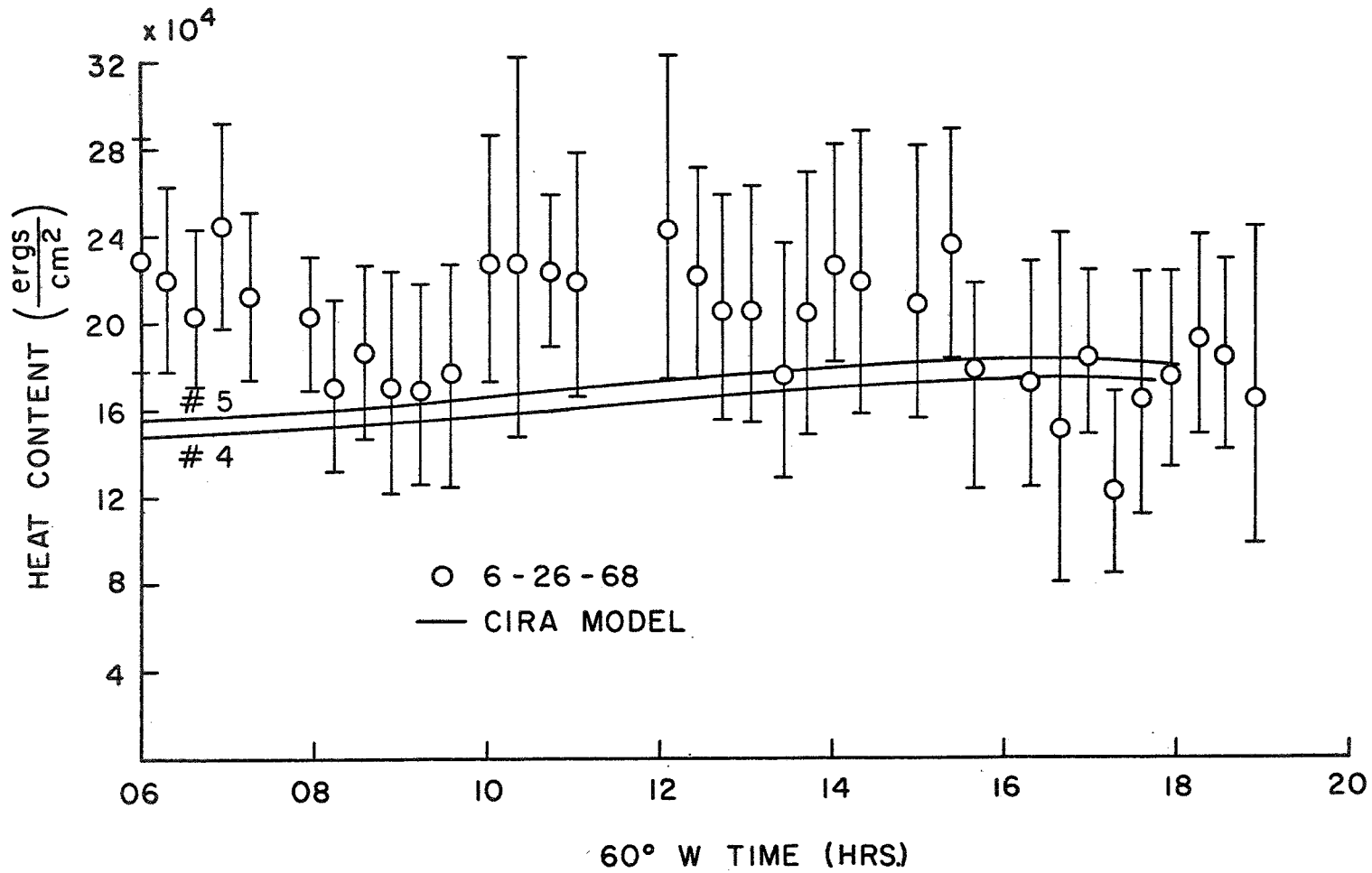


Figure 12  
Diurnal variation of the thermal energy column content  
for June 26, 1968 at Arecibo

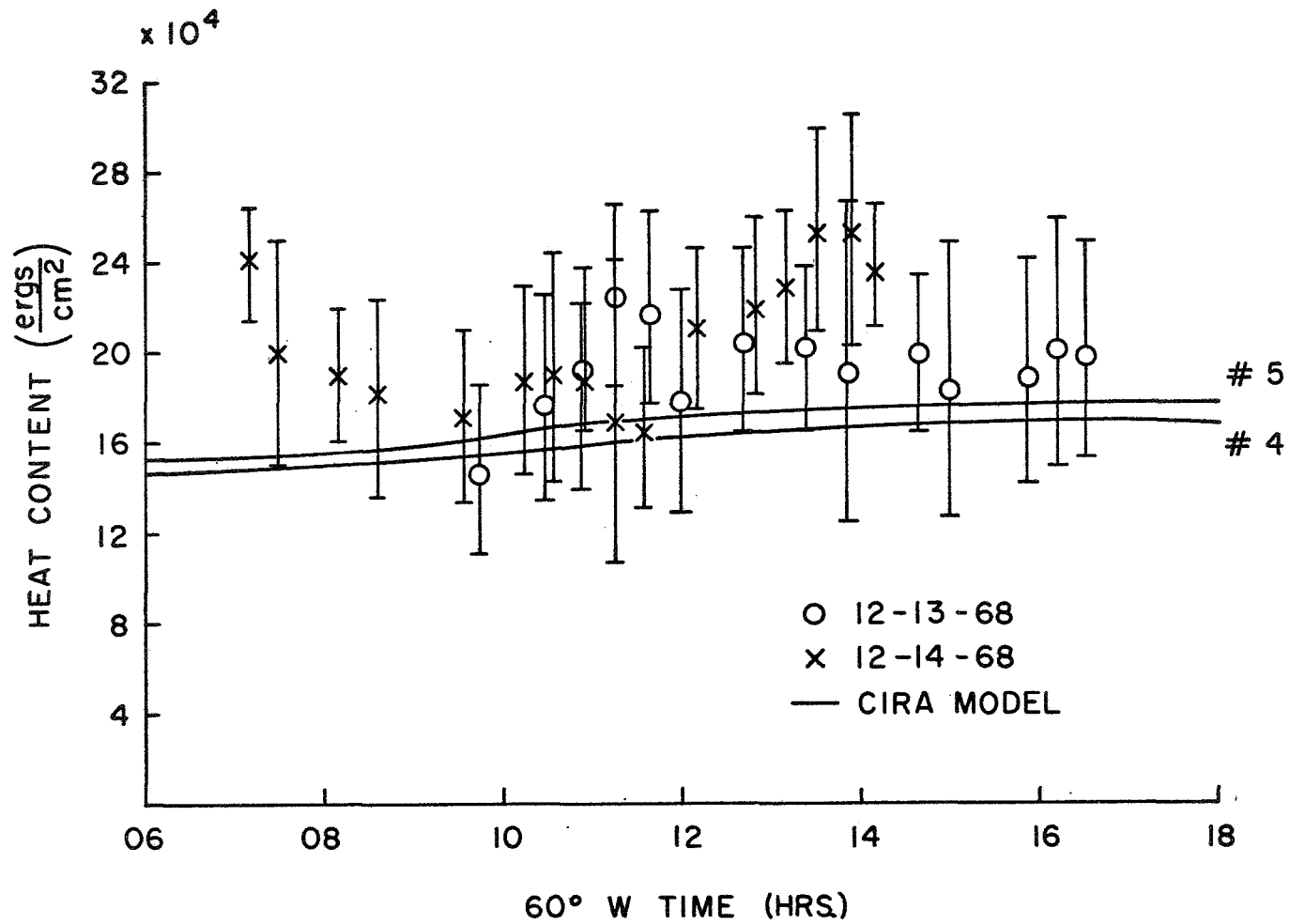


Figure 13.

Diurnal variation of the thermal energy column content for December 13 and 14, 1968 at Arecibo



nighttime heat source a heat content change of about  $3.5 \times 10^4$  ergs per  $\text{cm}^2$  in the 12 hour period from 1800 to 600 hours would be expected. This represents a fractional change in the evening heat content of some 20%. For the small sample of data thus far considered, this change does not appear likely and either the conduction drops off or there is some source of energy during the night. For the winter data the heat content at 1800 on December 13 is very nearly the same as at 600 on December 14, while the morning content on June 26 appears somewhat higher than in the evening. It is interesting to note that the preceding day's solar index was somewhat higher for the summer, whereas for the winter data the first day's index was lower and the change less. Such long term changes in the absence of a large change in the column content at night seem to imply a rather significant horizontal transport effect.

These results may usefully be compared with the assumptions of theoretical models of the upper atmosphere in which horizontal transport is neglected and in which the major source of energy loss above 120 km is conduction through the lower boundary. With such models the energy input during the day is greater than the heat conducted downwards to make up for the heat loss during the night. The heat content for such a model must be greatest at a time close to sunset. It may be noted that our observations in common with the CIRA (1965) and other models based on satellite orbital decay do not support this property of the one dimensional model. The observations still require considerable energy transport from the "afternoon" atmosphere to the "night" atmosphere.

## 4. CONCLUSIONS

### 4.1 The Diurnal Variations of the Upper Atmosphere

The high resolution measurements confirm previous results (Nisbet, 1967; Carru et. al., 1967; McClure, 1969) that the temperature  $T_n(\omega)$  does not decrease at Arecibo after 1400 hours as shown in the CIRA (1965) and Jacchia (1970 a, b) models but remains constant or increases slightly up to around sunset. The values of the exospheric temperature,  $T_n(\omega)$ , were also found to be lower than predicted by the CIRA (1965) model by about 30% and similar to the Jacchia (1970) model, except for the timing of the maximum. These results were shown to be quite insensitive to the assumptions about the lower boundary conditions on the atmospheric density.

While the densities at 300 km are quite dependent on those assumed at 120 km, it may be said that the mean value of the density at 300 km throughout the day as calculated in this work is comparable with the values for CIRA (1965) and higher than would be expected from the measured values of  $T_n(\omega)$ . The 300 km densities of the Jacchia (1970) model are also similar to the mean value presented here even though the diurnal behavior of the temperature was quite different. It was therefore demonstrated that there can be a significant phase difference between the density and temperature maxima of 3 to 5 hours which results from large changes in the gradients in the region from 120 to 150 km.

#### 4.2 Neutral Models Consistent with Incoherent Scatter Data

It has been shown that the complete plasma temperature profile with an assumption of diffusive equilibrium can be used to obtain consistent neutral temperatures and densities for the region above 120 km. By examining the physical characteristics of the resulting neutral temperature profiles for various values of the boundary density, it was possible to place a lower bound on the atomic oxygen density at 120 km of about  $5 \times 10^{10} \text{ cm}^{-3}$  while the best fit normally implied atomic oxygen densities greater than listed by CIRA (1965) and closer to those shown by Jacchia (1970). Such a best fit could only be obtained when the ion temperature departed significantly from the isothermal neutral temperatures in the higher altitudes. When the electron density became large in the afternoon the increased thermal coupling between the ions and neutrals reduced the temperature difference below the necessary level. Further calculations using incoherent scatter from higher altitudes coupled with simultaneous high resolution measurements at lower altitudes should provide a clear picture of the atomic oxygen variations at the 120 km level and greatly improve the accuracy of the neutral density measurements.

#### 4.3 The Energy Budget of the Model

Because of the complexity of the real situation, the unduly simple form of the assumed temperature profile cannot exactly satisfy the heat conduction equation even though it provides a good fit to the actual observed temperatures.

It may, however, be said that the observations are not consistent with a model in which horizontal transport is neglected and in which the main heat input is for EUV absorption and the main cooling from vertical conduction. The estimates of the total nighttime conduction through the 120 km level are too large for the observed changes in the thermal energy column content. Furthermore the content does not increase throughout the afternoon as would be expected of a model which can only transfer energy by downward conduction.

Some preliminary theoretical studies including winds have been made by Volland (1967, 1970), Friedman (1970), and Stubbe (1970), all of which implied the importance of horizontal transport although their specific conclusions were not completely consistent. A major problem in such theoretical analysis is the number of boundary conditions that have to be specified. It is hoped that the conclusions of the present work will, when subjected to experimental verification by other techniques, be helpful in the development of more realistic models.

#### 4.4 Suggestions for Further Work

Uncertainties in the neutral temperatures are due primarily to the errors in the ion temperatures. Since the plasma temperatures depend on the percentage compositions of the atomic and molecular ions, some uncertainty results directly from the estimates of the ion composition. This is especially true at sunrise when there are large neutral and plasma transport effects which may cause significant

departures from the assumed equilibrium conditions. Such errors in the temperatures within the molecular to atomic ion transition region are mainly projected into the parameter  $\tau$ .

Mass spectrometer measurements of both the neutral and ion densities and EUV spectrometric measurements of the solar flux made simultaneously with incoherent scatter observations including the plasma velocities will be important in better defining the temperatures in the transition region and thereby reduce the uncertainties in the temperature gradients which were encountered in the present analysis.

In the higher altitudes errors in the atomic oxygen density produce additional uncertainty in the neutral temperature profile through the parameter  $T_n(\infty)$ . If a satellite of suitable construction for orbital decay measurements preferably equipped with accelerometers were placed in an orbit with its perigee in the isothermal region above an incoherent scatter radar facility, this particular uncertainty could be reduced. This in turn would help to improve the density estimates near 120 km through its relation to the temperature profile, and provide a check on the neutral densities obtained directly from incoherent scatter data using both the spectral broadening caused by collisions in the lower altitudes and the best fit analysis described in this work.

While many data points in the present analysis contributed significantly to the search for  $T_n(\infty)$  with a fixed boundary density, only a few data points in the vicinity of 120 km contributed to  $T_n(Z_o)$ .

By increasing the resolution of the low altitude measurements, estimates of this parameter can be improved.

Being able to determine the boundary atomic oxygen density directly from the fitting procedure described in this work depends on a consistent departure of the ion temperature from the neutral temperature in the isothermal region of the upper altitudes. Often this difference was not greater than the scatter in the data for an altitude range large enough to give reliable densities. This problem could be remedied by simply extending the incoherent scatter measurements to higher altitudes and by taking careful account of the effects of the lighter ions.

Since the incoherent scatter radar facilities are the only instruments which can provide a continuous monitoring of the complete temperature profiles, it is important that the measurements by the several different methods available be made simultaneously and at the same general geographic location as the radars. Such correlated experiments will help eliminate any remaining instrumental discrepancies and be invaluable in providing the information necessary for specifying the behavior of the upper atmosphere.

## BIBLIOGRAPHY

- Banks, P., Collision frequencies and energy transfer: electrons, Planetary Space Sci., 14, 1085-1103, 1966.
- Banks, P., Collision frequencies and energy transfer: ions, Planetary Space Sci., 14, 1105-1122, 1966.
- Bates, D. R., Some problems concerning the terrestrial atmosphere above about the 100 km level, Proc. Roy. Soc., A253, 451-462, 1959.
- Bauer, P., P. Waldteufel, and D. Alcayde, Study of the Diurnal Variations of the Atomic Oxygen Density and Temperature Using Incoherent Scatter Measurements in the Ionospheric F Region, to be published in J. Geophysical Res., 1970.
- Biondi, M. A., Atmospheric electron-ion and ion-ion recombination processes, Canadian J. of Chemistry, 47 (10), 1711-1719, 1969.
- Blum, P. W., The delay between solar activity and density changes in the upper atmosphere, Planetary Space Sci., 16 (12), 1427-1440, December 1968.
- Broglio, L., Air density between 200 and 300 km obtained by San Marco 1 Satellite, Space Res. VII, ed. by R. L. Smith-Rose, S. A. Bowhill, and J. W. King (North-Holland Pub. Co., Amsterdam), 1135-1147, 1967.
- Byram, E. T., T. A. Chubb, and H. Friedman, The solar X-ray spectrum and the density of the upper atmosphere, J. Geophysical Res., 61(2), 251-263, 1956.
- Carru, H., M. Petit, G. Vasseur, P. Waldteufel, Resultats ionospheriques obtenus par diffusion de Thompson, Annales de Geophysique, 23(4), 455-465, 1967.
- Chandra, S., and P. Stubbe, The diurnal phase anomaly in the upper atmospheric density and temperature, to be published in Planetary Space Sci., 1970.
- Champion, K. S. W., Variations with season and latitude of density, temperature, and composition in the lower thermosphere, Space Res. VII, ed. by R. L. Smith-Rose (North-Holland Pub. Co., Amsterdam), 1101-1118, 1968.
- Colegrove, F. D., F. S. Johnson, and W. B. Hanson, Atmospheric composition in the lower thermosphere, J. Geophysical Res., 71(9), 2227-2236, May 1, 1966.

- Cook, G. E., Satellite drag coefficients, Planetary Space Sci., 13, 929-946, 1965.
- Cook, G. E., Drag coefficients of spherical satellites, Annales de Geophysique, 22(1), 53-64, 1966.
- Cook, G. E., The semi-annual variation in the upper atmosphere: A review, Annales de Geophysique, 25(2), 451-469, 1969.
- Cook, G. E., D. B. King-Hele, and D. M. C. Walker, The contraction of satellite orbits under the influence of air drag, I. With spherically symmetric atmosphere, Proc. Roy. Soc. (London), A257, 224-249, September 27, 1960.
- Cook, G. E., D. G. King-Hele, and D. M. C. Walker, The contraction of satellite orbits under the influence of air drag, II. With oblate atmosphere, Proc. Roy. Soc. (London), A264, 88-121, October 24, 1961.
- Danilov, A. D., Composition of the atmosphere in the 100-200 km region, NASA Technical Translation F-389, 1965.
- Friedman, M. P., A three-dimensional model of the upper atmosphere, Smithsonian Astrophys. Obs., Spec. Rpt. No. 250, 1-101, September 19, 1967.
- Friedman, M. P., Upper atmosphere dynamics, Smithsonian Astrophys. Obs., Spec. Rpt. No. 316, 1-52, May 28, 1970.
- Hall, L. A., C. W. Chagnon, and H. E. Hinteregger, Daytime variations in the composition of the upper atmosphere, J. Geophysical Res., 72(13), 3425-3427, July 1, 1967.
- Hall, L. A., K. R. Damon, and H. E. Hinteregger, Solar extreme ultraviolet photon flux measurements in the upper atmosphere of August 1961, Space Res. III, ed. by W. Priester (North-Holland Pub. Co., Amsterdam), 745-771, 1963.
- Hall, L. A., J. E. Higgins, C. W. Chagnon, and H. E. Hinteregger, Solar-cycle variation of extreme ultraviolet radiation, J. Geophysical Res., 74(16), 4181-4183, 1969.
- Hall, L. A., W. Schweizer, and H. E. Hinteregger, Diurnal variation of the atmosphere around 190 kilometers derived from solar extreme ultraviolet absorption measurements, J. Geophysical Res., 68, 6413-6417, 1963.
- Hall, L. A., W. Schweizer, and H. E. Hinteregger, Improved extreme ultraviolet absorption measurements in the upper atmosphere, J. Geophysical Res., 70, 105-111, 1965.



- Harris, I. and W. Priester, Time-dependent structure of the upper atmosphere, NASA Technical Note D-1443, 1-71, July 1962.
- Harris, I., and W. Priester, Theoretical models for the solar-cycle variation of the upper atmosphere, J. Geophysical Res., 67(12), 4585-4591, November 1962.
- Hedin, A. E., and A. O. Nier, A determination of the neutral composition, number density, and temperature of the upper atmosphere from 120 to 200 kilometers with rocket-borne mass spectrometers, J. Geophysical Res., 71(17), 4121-4131, September 1, 1966.
- Hinteregger, H. E., Telemetering monochrometer measurements of extreme ultraviolet radiation, Space Astrophysics, ed. by W. Liller (McGraw Hill Book Co., N. Y.), 34-95, 1961.
- Hinteregger, H. E., Preliminary data on solar extreme ultraviolet radiation in the upper atmosphere, J. Geophysical Res., 66(8), 2367-2380, August 1961.
- Hinteregger, H. E., Absolute intensity measurements in the extreme ultraviolet spectrum of solar radiation, Space Science Rev., 4(4), 462-497, June 1965.
- Hinteregger, H. E., Effects of solar XUV-radiation on the earth's atmosphere, IQSY/COSPAR Symposium, London, paper III-1, 1967.
- Hinteregger, H. E., K. R. Damon, L. Heroux, and L. A. Hall, Telemetering Monochrometer measurements of solar 304 Å radiation and its attenuation in the upper atmosphere, Space Res. I, ed. by H. Kallmann-Bijl (North-Holland Pub. Co., Amsterdam) 615-627, 1960.
- Hinteregger, H. E., L. A. Hall, and G. Schmidke, Solar EUV radiation and neutral particle distribution in July 1963, Space Res. V, ed. by D. G. King-Hele, P. Muller, and G. Righini (North-Holland Pub. Co., Amsterdam), 1175-1190, 1965.
- Horowitz, R., Direct measurements of density in the thermosphere, Annales de Geophysique, 22(1), 31-39, 1966.
- Jacchia, L. G., A variable atmospheric-density model from satellite accelerations, Smithsonian Astrophys. Obs., Spec. Rpt. No. 39, March 30, 1960.
- Jacchia, L. G., A working model for the upper atmosphere, Nature, 192, 1147-1148, December 23, 1961.

- Jacchia, L. G., The temperature above the thermopause, Space Res. V, ed. by P. Muller (North-Holland Pub. Co., Amsterdam), T152-1175, 1965; Also in Smithsonian Astrophys. Obs. Spec. Rpt. No. 150, 1-32, April 22, 1964.
- Jacchia, L. G., Static diffusion models of the atmosphere with empirical temperature profiles, Smithsonian Contr. Astrophys., 8, 215-257, 1965; Also in Smithsonian Astrophys. Obs. Spec. Rpt. No. 170, December 1964.
- Jacchia, L. G., Density variations in the heterosphere, Annales de Geophysique, 22(1), 75-85, 1966.
- Jacchia, L. G., Recent results in the atmospheric region above 200 km and comparisons with CIRA 1965, Space Res. VIII, ed. by A. P. Mitra, L. G. Jacchia, and W. S. Newman (North-Holland Pub. Co., Amsterdam), 800-810, 1968; Also in Smithsonian Astrophys. Obs. Spec. Rpt. No. 245, 25 pp., 1967.
- Jacchia, L. G., New static models of the thermosphere and exosphere with empirical temperature profiles, Smithsonian Astrophys. Obs. Spec. Rpt. No. 313, 1-88, May 6, 1970.
- Jacchia, L. G., Private Communication, July 16, 1970.
- Jacchia, L. G., and J. W. Slowey, Short-period oscillations in the drag of satellite 1958 Alpha, Smithsonian Contr. Astrophys., 6, 199-204, 1963.
- Jacchia, L. G., and J. Slowey, Accurate drag determinations for eight artificial satellites; atmospheric densities and temperatures, Smithsonian Contr. Astrophys., 8(1), 1-99, 1963.
- Jacchia, L. G., and J. Slowey, An analysis of the atmospheric drag of the explorer IX satellite from precisely reduced photographic observations, Smithsonian Astrophys. Obs. Spec. Rpt. No. 125, 1-57, May 28, 1963.
- Jacchia, L. G., and J. Slowey, Atmospheric heating in the auroral zones: A preliminary analysis of the atmospheric drag of the Inju 3 satellite, J. Geophysical Res., 69(5), 905-910, March 1, 1964.
- Jacchia, L. G., and J. Slowey, Temperature variations in the upper atmosphere during geomagnetically quiet intervals, J. Geophysical Res., 69(19), 4145-4148, October 1, 1964.
- Jacchia, L. G., and J. Slowey, The shape and location of the diurnal bulge in the upper atmosphere, Space Res. VII, ed. by R. L. Smith-Rose, C. A. Bowhill, and J. W. King (North-Holland Pub. Co., Amsterdam), 1077-1090, 1967.

- Jacchia, L. G., and J. W. Slowey, Diurnal and seasonal latitudinal variations in the upper atmosphere, Planetary Space Sci., 16(4), 509-524, April 1968.
- Jastrow, R., and C. A. Pearse, Atmospheric drag on the satellite, J. Geophysical Res., 62, 413-423, 1967.
- Johnson, F. S., Temperatures in the high atmosphere, Annales de Geophysique, 14(1), 94-107, 1958.
- Kasprzak, W. T., D. Krankowsky, and A. O. Nier, A study of day-night variations in the neutral composition of the lower thermosphere, J. Geophysical Res., 73(21), 6765-6782, November 1, 1968.
- Kasner, W. H., and M. A. Biondi, Electron-ion recombination studies in oxygen, Bull. A. Phys. Soc., 12, 218, 1967.
- King-Hele, D. G., Decrease in upper-atmosphere density since the sunspot maximum of 1957-58, Nature, 198, 832-834, 1963.
- King-Hele, D. G., Methods of determining air density from satellite orbits, Annales de Geophysique, 22(1), 50-52, 1966.
- King-Hele, D. B., and E. Quinn, The variation of the upper atmosphere density between sunspot maximum (1957-1958) and minimum (1964), J. Atmospheric and Terrestrial Phys., 27, 197-209, 1965.
- King-Hele, D. G., and J. Hingston, Variations in air density at heights near 150 km, from the orbit of the satellite 1966-101G, Planetary Space Sci., 15(2), 1883-1893, December 1967.
- Kockarts, G., Mean molecular mass and scale heights of the upper atmosphere, Annales de Geophysique, 22(2), 161-174, 1966.
- Krankowsky, D., W. T. Kasprzak, and A. O. Nier, Mass spectrometric studies of the composition of the lower thermosphere during summer 1967, J. Geophysical Res., 73(23), 7291-7302, December 1968.
- Krassovsky, V. I., Exploration of the upper atmosphere with the help of the third Soviet sputnik, Proc. IRE, 41, 289-295, 1959.
- Landini, M., D. Russo, and G. S. Tagliaferri, Atmospheric density in the 120-190 km region derived from the X-ray extinction measured by the U. S. Naval Research Laboratory satellite 1964-01-D, Nature, 206(4980), 173-174, April 1965.

- Marov, M. Y., The density of the upper atmosphere, Annales de Geophysique, 22(1), 65-74, 1966.
- Mauersberger, K., D. Muller, D. Offermann, and U. VonZahn, A mass spectrometer determination of the neutral constituents in the lower thermosphere above Sardinia, J. Geophysical Res., 73(3), 1071-1076, February 1, 1968.
- Mauersberger, K., D. Muller, D. Offermann, and U. VonZahn, Neutral constituents of the upper atmosphere in the altitude range of 110 to 160 km above Sardinia, Space Res. VII, ed. by R. S. Smith-Rose (North-Holland Pub. Co., Amsterdam), 1150-1158, 1968.
- McClure, J. P., Diurnal variation of neutral and charged particle temperature in the equatorial F-region, J. Geophysical Res., 74(1), 279-291, 1969.
- Meier, R. R., Temporal variations of solar Lyman alpha, J. Geophysical Res., 74(26), 6487-6490, 1969.
- Moe, K., D. Klein, G. Maled, and L. Tsang, Density scale heights at sunspot maximum and minimum from satellite data, Planetary Space Sci., 16(4), 409-417, April 1968.
- Newton, G. P., Changes in atmospheric density variations with latitude, Paper presented at the 15th annual meeting AGU, Washington, D. C., April 1969.
- Newton, G. P., and D. T. Pelz, Latitudinal variations in the neutral atmospheric density, J. Geophysical Res., 74(16), 4169-4174, August 1, 1969.
- Nicolet, M., Actions du rayonnement solaire dans la haute atmosphere, Annales de Geophysique, 8(2), 141-193, 1952.
- Nicolet, M., Dynamic effects in the high atmosphere. In The Earth as a Planet, ed. by G. P. Kuiper (Univ. Chicago Press, Chicago), 644-712, 1954.
- Nicolet, M., La thermosphere, Annales de Geophysique, 15(1), 1-22, January 1959.
- Nicolet, M., The constitution and composition of the upper atmosphere, Proc. IRE, 47(2), 142-147, February 1959.
- Nicolet, M., The properties and constitution of the upper atmosphere, Physics of the Upper Atmosphere, ed. by J. A. Ratcliffe (Academic Press, New York), 17-71, 1960.

- Nicolet, M., Les variations de la densite et du transport de chaleur par conduction dans l'atmosphere superieure, Space Res. I, ed. by H. Kallmann-Bijl (North-Holland Pub. Co., Amsterdam), 46-89, 1960.
- Nicolet, M., Density of the heterosphere related to temperature, Smithsonian Contr. Astrophys., 6, 175-187, 1963; Also in Smithsonian Astrophys. Obs. Spec. Rpt. No. 75, 1-30, 1961.
- Nicolet, M., A representation of the terrestrial atmosphere from 100 km to 3000 km, Ionosphere Research Sci. Rpt. No. 155, The Pennsylvania State University, February 1, 1962.
- Nicolet, M., Solar radio flux and temperature of the upper atmosphere, J. Geophysical Res., 68, 6121-6144, 1963.
- Nier, A. O., The neutral composition of the thermosphere, Annales de Geophysique, 22(1), 102-109, 1966.
- Nier, A. O., J. H. Hoffman, C. Y. Johnson, and J. C. Holmes, Neutral composition of the atmosphere in the 100-to-200 kilometer range, J. Geophysical Res., 69, 979-989, 1964.
- Nisbet, J. S., Neutral atmospheric temperature from incoherent scatter observations, J. Atmospheric Sciences, 24(5), 586-593, 1967.
- Nisbet, J. S., On the construction and use of simple ionospheric models, paper presented at the 1969 Spring URSI meeting in Washington, D. C., April 22, 1969.
- Paetzold, H. K., and H. Zschorner, The structure of the upper atmosphere and its variations after satellite observations, Space Res. II, ed. by H. C. Van de Hulst, C. de Jager, and A. F. Moore (North-Holland Pub. Co., Amsterdam), 958-973, 1961.
- Pokhunkov, A. A., Mass spectrometer investigation of the neutral composition of the upper atmosphere, Annales de Geophysique, 22(1), 92-101, 1966.
- Pokhunkov, A. A., Mass spectrometer measurements of the upper atmosphere temperature, Space Res. VII, ed. by R. S. Smith-Rose (North-Holland Pub. Co., Amsterdam), 1159-1166, 1968.
- Priester, W., M. Roemer, and H. Volland, The physical behavior of the upper atmosphere deduced from satellite drag data, Space Sci. Rev., 6, 707-780, 1967.
- Roemer, M., Geomagnetic activity effect and 27-day variation: Response time of the thermosphere and lower exosphere, Space Res. VII, ed. by R. S. Smith-Rose (North-Holland Pub. Co., Amsterdam), 1091-1099, 1968.

- Roemer, M., Structure of the thermosphere and its variations, Annales de Geophysique, 25(2), 419-437, 1969.
- Shimazaki, T., Dynamic effects on height distributions of diurnal constituents in the earth's upper atmosphere: A calculation of atmospheric model between 70 km and 500 km, J. Atmospheric Terrestrial Phys., 30, 1279-1292, 1968.
- Spencer, N. W., L. H. Brace, G. R. Carignan, D. R. Tausch, and H. Niemann, Electron and molecular nitrogen temperature and density in the thermosphere, J. Geophysical Res., 70(11), 2665-2698, June 1, 1965.
- Spencer, N. W., and C. A. Reber, A mass spectrometer for an aeronomy satellite, Space Res. III, ed. by W. Priester (North-Holland Pub. Co., Amsterdam), 1151-1155, 1963.
- Spencer, N. W., D. R. Tausch, and G. R. Carignan, N<sub>2</sub> temperature and density data for the 150-300 km region and their implications, Annales de Geophysique, 22, 151-160, 1966.
- Stein, J. A., and J. C. G. Walker, Models of the upper atmosphere for a wide range of boundary conditions, J. Atmospheric Sciences, 22, 11-17, 1965.
- Sterne, T. E., An atmospheric model, and some remarks on the inference of density from the orbit of a close earth satellite, Astronomical J., 63, 81- , 1958.
- Stubbe, P., Simultaneous solution of the time dependent coupled continuity equations, heat conduction equations, and equations of motion for a system consisting of a neutral gas, an electron gas, and a four component ion gas, J. Atmospheric Terrestrial Phys., 32, 865-903, 1970.
- Swenson, G. R., Temperature shape parameter of the thermosphere determined from probe data, J. Geophysical Res., 74(16), 4074-4078, August 1, 1969.
- Tausch, D. R., H. B. Niemann, G. R. Carignan, R. E. Smith, and J. O. Ballance, Diurnal survey of the thermosphere (1) neutral particle results, Space Res. VIII, ed. by A. P. Mitra, L. G. Jacchia, and W. S. Newmann (North-Holland Pub. Co., Amsterdam), 930-939, 1968.
- Thomas, L., F. H. Venables, and K. M. Williams, Measurements of solar X-ray fluxes by the U. S. Naval Research Laboratory satellite 1964-01-D, Planetary Space Sci., 13, 807-833, 1965.

- Venables, F. H., Solar X-rays in the wavelength band 44-60 Å<sup>0</sup> observed by the U. S. satellite 1965-16D and atmospheric optical densities deduced from these observations, Planetary Space Sci., 15, 681-688, 1967.
- Volland, H., On the dynamics of the upper atmosphere, Space Res. VII, ed. by R. L. Smith-Rose (North-Holland Pub. Co., Amsterdam), 1193-1203, 1967.
- Volland, H., A theory of thermospheric dynamics - I: Diurnal and solar cycle variations, Planetary Space Sci., 17, 1581-1597, 1969.
- Weidner, D. K., and G. R. Swenson, Diurnal variations in the thermosphere from a series of Marshall-University-of-Michigan probes, J. Geophysical Res., 74(19), 4755-4764, September 1, 1969.
- Weller, C. S. and M. A. Biondi, Temperature dependence of recombination of NO<sup>+</sup> ions and electrons, Bull. Am. Phys. Soc., 13, 199, 1968.